Glacial history of the King Haakon trough system, sub-Antarctic South Georgia

Katharina Teresa Streuff [a,b,*], Nina-Marie Lešić [a,b,c], Gerhard Kuhn [a,c], Miriam Römer [a,b], Sabine Kasten [a,b,c], Gerhard Bohrmann [a,b]

[a] *University of Bremen, Faculty of Geosciences, Klagenfurter Straße 2-4, 28359, Bremen, Germany*
[b] *MARUM – Center for Marine Environmental Sciences, University of Bremen, Leobener Straße 8, 28359, Bremen, Germany*
[c] *Alfred Wegener Institute Helmholtz Centre for Polar and Marine Research, Am Handelshafen 12, 27570, Bremerhaven, Germany*

ARTICLE INFO

ABSTRACT

The glaciated island of South Georgia in the sub-Antarctic is a key area for climate reconstructions, because it is positioned in the Southern Ocean amidst the core belt of the Southern Westerlies and the main fronts of the Antarctic Circumpolar Current. This makes it particularly susceptible to changes in local, regional, but also Southern Hemisphere-wide climate conditions. Marine-geological records recovered from its continental shelf therefore offer unique potential to constrain how ice masses in this part of the Southern Ocean responded to Quaternary climate change, but despite this, little glacial-geomorphological and sedimentological research has been done offshore South Georgia. Here, we present a new suite of glacial landforms, identified from high-resolution bathymetry data, supplemented with acoustic facies from sub-bottom profiles, in order to reconstruct the pre-Holocene glacial history of the King Haakon Trough System on the southwestern South Georgia continental shelf. Our data show numerous landforms common for phases of ice advance and retreat, which are interpreted to document the confluence of two major trunk glaciers during peak glaciation. Progressively elongated linear bedforms imply accelerated ice flow and/or softer sediment substrate towards the shelf edge and suggest that the South Georgia Ice Cap experienced streaming ice and behaved similarly to other palaeo-ice sheets. A grounding-zone wedge close to the shelf edge marks the position of maximum ice extent during a peak glaciation, while clusters of recessional moraines and three large morainal banks indicate repeated phases of staggered retreat. Multiple extensive ice advances are indicated by stacked till sequences within the sub-bottom profiles of the mid- and outer shelf. The second-to-last till generation appears to be slightly more extensive than the most recent glacial till, and could suggest that South Georgia may have had a similar glacial evolution to other sub-Antarctic islands. This paper complements two studies focusing on the Holocene depositional environments and their associated sedimentary processes in the same trough system, in an effort to elucidate an important part of the Quaternary evolution of South Georgia's marine environment.

1. Introduction

The geomorphology of previously glaciated regions offers valuable insights into past ice sheet behaviour, because glacially modified landscapes act as an archive for glacial footprints. The (palaeo-)bed surface, especially in the marine environment, often hosts a plethora of glacial landforms, which can be used to spatially reconstruct specific ice sheet configurations (e.g. Evans et al., 2004; Ottesen et al., 2005; Andreassen et al., 2008; Bradwell et al., 2008; Ottesen and Dowdeswell, 2009; Dowdeswell et al., 2016b; Arndt et al., 2017), phases of advance/retreat (e.g. Ó Cofaigh et al., 2002; Dowdeswell et al., 2007; Dowdeswell et al., 2008b; Andreassen et al., 2014; Ottesen et al., 2017; Streuff et al., 2017a), and maximum ice extent (e.g. Clark et al., 2012; Arndt et al., 2015; Brouard and Lajeunesse, 2017; Dowdeswell et al., 2020). Similarly, sediment sequences observed on shallow seismic profiling allow for the interpretation of past sedimentary environments and associated depositional processes, especially when verified with sediment cores (e.g. Ó Cofaigh et al., 2008; Forwick and Vorren, 2009, 2011; Hogan et al.,

2011; Streuff et al., 2017a, 2018). Glacial cross-shelf troughs, often deeply eroded, are of particular importance in this regard, as they provide accommodation space for glacial and deglacial sediment sequences, and are therefore rare and valuable archives for palaeoenvironmental proxies in glaciated areas.

Reconstructions such as those outlined above are needed to improve modelling efforts, which aim to illustrate the potential ramifications of Earth's two largest remaining ice sheets, the Greenland and the Antarctic Ice Sheet, melting in response to a warming climate. Although the investigation of glacial geomorphology, in combination with radiocarbon dating, has been used to successfully reconstruct palaeo-ice sheets across the Northern Hemisphere (e.g. Ottesen et al., 2007; Clark et al., 2012; Hughes et al., 2016), as well as large parts of Antarctica (e.g. Anderson et al., 2014; Bentley et al., 2014; Hillenbrand et al., 2014; Larter et al., 2014; Mackintosh et al., 2014; Ó Cofaigh et al., 2014; Klages et al., 2015), the glacial history of the sub-Antarctic islands remains exceptionally poorly constrained (Bentley et al., 2014; Hodgson et al., 2014b; Graham et al., 2017). Situated in the Polar Frontal Zone, however, these islands have undergone considerable environmental change in the past and can therefore provide critical information on climate drivers affecting past and future ice-sheet change in the Southern Hemisphere (van der Putten et al., 2009; Hodgson et al., 2014b; White et al., 2017).

In this context, the island of South Georgia is a valuable research target. It is located in the Southern Ocean within two large climatic features, the Southern Hemisphere Westerly Winds (Westerlies) and the Antarctic Circumpolar Current (ACC), both of which impact the climate in the Southern Hemisphere and Antarctica (Strother et al., 2015; Moreno et al., 2018; Matano et al., 2020; Bakke et al., 2021). Since ice masses in the sub-Antarctic have been amongst the earliest to respond to recent global warming (e.g. Gordon et al., 2008; Cook et al., 2010), marine archives from, e.g. South Georgia, yield crucial information not only about the interactions between climate and ice sheet stability (Hodgson et al., 2014b), but also about past climate configuration. Locally, they inform about past ice extent, which allows for conclusions about parameters such as regional shelf current configurations and relative air and ocean temperatures (e.g. Graham et al., 2017; Lešić et al., 2024). Regionally, they can enable the reconstruction of past configurations of the ACC, relative current strength, previous locations of the Polar Front, as well as the relative strength of the Westerlies across the Southern Hemisphere (e.g. Pudsey and Howe, 1998; Bianchi and Gersonde, 2004; Wu et al., 2021; Lešić et al., 2024). And on a global scale, they will provide further knowledge on climate synchronicity, not only between different regions in the sub-Antarctic, but also between the Northern and the Southern Hemisphere (cf. bipolar see-saw; Broecker, 1998; Blunier and Brook, 2001).

Despite its potential, relatively few studies exist on South Georgia, most of which have been carried out in the terrestrial or near-shore realm of a smaller region in its northeast (e.g. Rosqvist et al., 1999; van der Putten and Verbruggen, 2005; Oppedal et al., 2018; Berg et al., 2019; Bakke et al., 2021). The dearth of chronological information, combined with contrasting data from terrestrial, coastal, and marine environments, has led to different interpretations regarding past ice extents (e.g. Barlow et al., 2016; Barnes et al., 2016; Graham et al., 2017). This raised, rather than answered, questions about the maximum extent of the South Georgia Ice Cap (SGIC) not only during the Local Last Glacial Maximum (LLGM; cf. Clark et al., 2009), but also during preceding glaciations. Although the large-scale glacial history as well as the more recent ice dynamics in some fjords have been roughly reconstructed (Graham et al., 2008, 2017), the majority of the numerous cross-shelf troughs, with the exception of Drygalski Trough in the southeast of South Georgia (Lešić et al., 2022), remain unstudied in terms of their glacial evolution during and since the LLGM. This study presents hydroacoustic data from a large and complex cross-shelf trough system, the King Haakon Trough System, on the southwestern continental shelf of South Georgia (Fig. 1). By describing and interpreting the

glacial footprints recorded in bathymetry and sub-bottom profiler data, we aim to elucidate the glacial history of one of the, presumably major, pathways, carved into the continental shelf during past glacial periods. Focusing exclusively on the trough evolution prior to ~10 ka BP, this paper complements two studies by Lešić et al. (one published in 2024, one forthcoming) on the Holocene depositional environments in the same trough. It will, therefore, make a valuable contribution to the, thus far very limited, glacial-geomorphological and sedimentological literature about the continental shelf around South Georgia.

2. Physiographic setting

South Georgia is one of the largest islands in the sub-Antarctic and is located in the Atlantic sector of the Southern Ocean, between 54° and 55° S and 35°30' and 38° W (Fig. 1). It is geologically a microcontinent (Dalziel et al., 2021), which is unique in terms of a very large continental shelf, that is roughly ten times larger than the island itself. The island has a sub-polar maritime and cool climate and is still heavily glacierized, with the majority of glaciers considered as temperate (e.g. Smith, 1960). Bathymetric data have revealed a number of large cross-shelf troughs that spread, mostly radially, from the coast to the continental shelf edge, and have been interpreted as the product of large ice streams draining the SGIC during past glacial periods (Fig. 1b; Graham et al., 2008, 2017). King Haakon Trough (KHT) is one of these and is located on the southwestern South Georgia continental shelf (Fig. 1b). Because it is joined by several other troughs, including Jacobsen and Annenkov Troughs (nomenclature according to Bohrmann et al., 2017), it has previously been defined as the King Haakon Trough System (KHTS; Fig. 1b and c; Lešić et al., 2024).

KHTS is up to 14 km wide, about 80 km long from coast to shelf edge, and up to 400 m deep (Fig. 1c). It consists of the main, N–S oriented trough valley of KHT, and two main tributaries, Jacobsen Trough (JT) and Annenkov Trough (AT) joining it from the east at a distance of approximately 12 km from the coast (Fig. 1c). KHT is fed by Cheapman, King Haakon, and Queen Maud Bays from the north (Fig. 1c) with all inlets hosting a minimum of one marine-terminating glacier. Peters and Price Glaciers feed into Cheapman Bay, while Briggs Glacier, an outlet of the Murray Snowfield, drains into King Haakon Bay, and Hawkesbury Glacier terminates in Queen Maud Bay (Fig. 1c; nomenclature after South Georgia GIS, 2023).

JT and AT are separated by a prominent bathymetric high (BH1) located ~4.5 km east of the confluence zone with KHT (Figs. 1c, 2). Both troughs are joined by several tributary bays from the north and northeast, which include Jossac Bight, Newark Bay, and Jacobsen Bight (Fig. 1c). All JT tributaries also have a number of marine-terminating glaciers at their heads, including Esmark, Keilhau and Jewell Glaciers in Jossac Bight, Lancing, Christensen and Kjerulf Glaciers in Newark Bay, and Eclipse, Christophersen and Bary Glaciers for Jacobsen Bight (Fig. 1c). JT and AT, in combination with their three tributaries, have previously been referred to as the Jacobsen Trough System (JTS; Lešić et al., 2024).

The tributaries joining KHT and JT show distinct differences in their appearance. Although bathymetric data for many of the coastal regions of South Georgia is still very poorly resolved for the most part, aerial imagery as well as compiled bathymetry data (including datasets by Hodgson et al., 2014a; Hogg et al., 2016, 2017, and the General Bathymetric Chart of the Oceans by the GEBCO Compilation Group, 2023) show that King Haakon Bay, with a length of ~13 and a width of up to 3 km, a fjord basin and an outer sill/moraine, has characteristics of a typical fjord, and is similar to other major fjords in South Georgia (Hodgson et al., 2014a). King Haakon Bay is orientated predominantly E-W, i. e. perpendicular to the major trough basin of KHT (Fig. 1). Cheapman and Queen Maud Bays, while also "fjord-like" in appearance, are smaller embayments with a shorter, more open morphology (Fig. 1c). Similarly, the tributaries of JT are much shorter (mostly <3 km) than King Haakon Bay, and appear to be wider and more open.
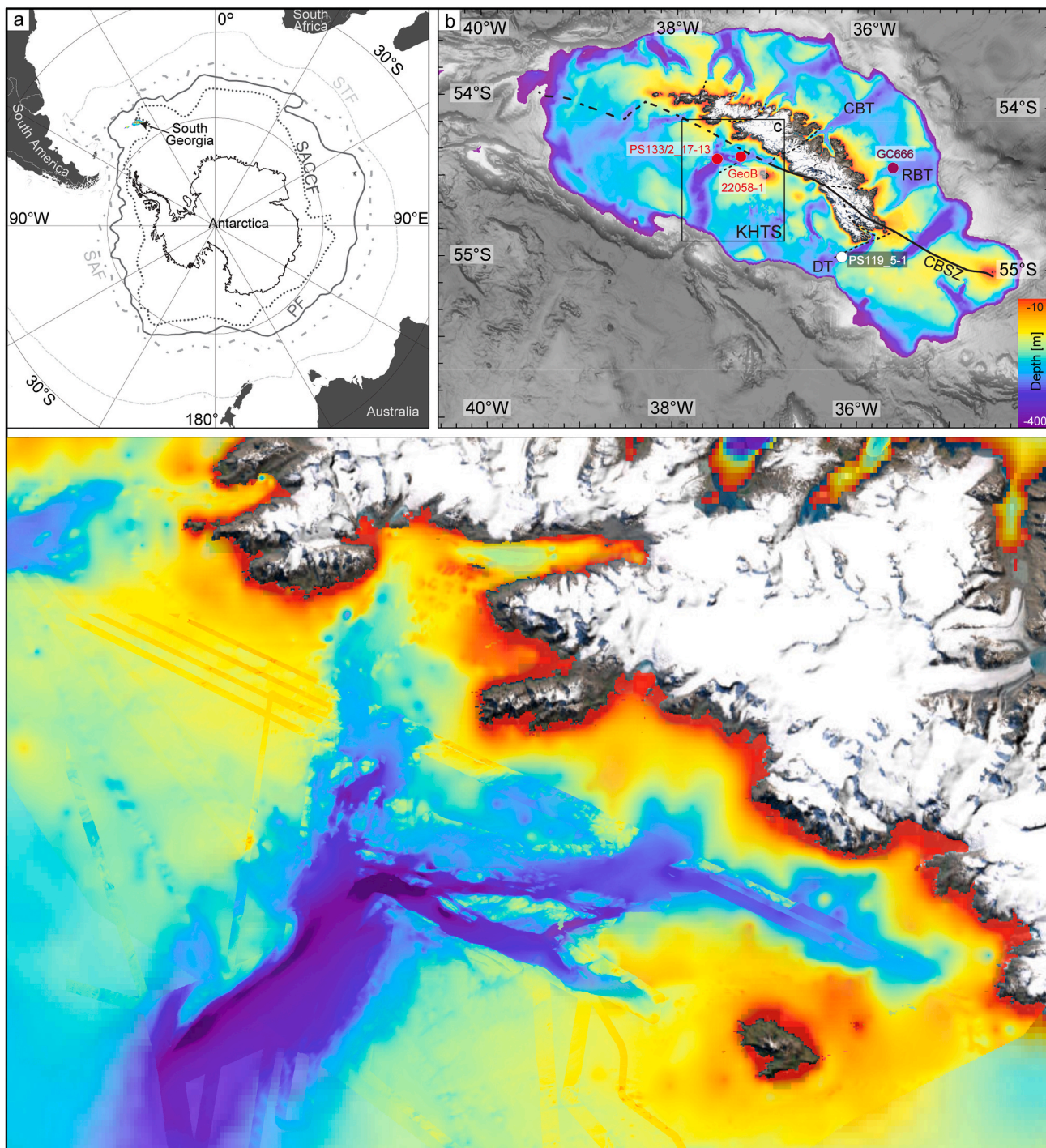
Fig. 1. a) Location of South Georgia in the Southern Ocean with respect to the different oceanographic fronts, based on Orsi et al. (1995). STF = Subtropical Front, SAF = Sub-Antarctic Front, PF = Polar Front, and SACCF = Southern Antarctic Circumpolar Current Front. b) Marine environment around South Georgia with the thus far investigated troughs. DT = Drygalski Trough, RBT = Royal Bay Trough, and CBT = Cumberland Bay Trough. The continental shelf is defined as the area between 0 and 400 m water depths and depicted in colour. Bathymetry in water depths >400 m is depicted with a greyscale hillshade. The location of the study area (King Haakon Trough System; KHTS) is indicated by the black rectangle. The major fault zone, the Cooper Bay Shear Zone (CBSZ, Dalziel et al., 2021) runs ENE-WSW across the southern part of the island. Several additional faults (black dotted lines) were inferred by Graham et al. (2008). Dots show four sediment core sites, from where radiocarbon dates have been published, with PS133/2_17–13 and GeoB22058-1 in KHTS (red, Lešić et al., 2024), PS119_5–1 in DT (green, Lešić et al., 2022) and GC666 in RBT (purple, Graham et al., 2017). Bathymetric data from GEBCO Compilation Group (2023) and Hogg et al. (2017), with the island illustrated as per the ArcMap™ imagery basemap. c) Overview of KHTS with all troughs and tributaries. Core sites indicated in b) are shown as black circles. Marine-terminating glaciers along the coast are 1 = Peters Glacier, 2 = Price Glacier, 3 = Briggs Glacier, 4 = Hawkesbury Glacier, 5 = Esmark Glacier, 6 = Keilhau Glacier, 7 = Jewell Glacier, 8 = Lancing Glacier, 9 = Christensen Glacier, 10 = Kjerulf Glacier, 11 = Eclipse Glacier, 12 = Christophersen Glacier. Nomenclature from South Georgia GIS (2023). The Jacobsen Trough System consists of Jacobsen Trough (JT), Annenkov Trough (AT) as well as the tributaries. Throughout this study we will also use the terms northern, central and outer King Haakon Trough (KHT) and inner, mid- and outer shelf, which are marked here for reference.

Although the GEBCO and Hogg et al. (2016, 2017) data rely largely on interpolation and may thus not be too reliable this close to the coast, the bathymetric information also seems to indicate a relatively shallow seafloor and an associated lack of fjord basins and sills/moraines for the JTS tributaries (Fig. 1c).

3. Methods

Bathymetric and sediment echosounder data were gathered opportunistically during two separate cruises, namely expedition M134 on *RV Meteor* in 2017 (Bohrmann et al., 2017) and expedition PS133/2 on *RV Polarstern* in 2022 (Kasten, 2023). Onboard the *Meteor,* bathymetric data were predominantly acquired using the Kongsberg Maritime EM710 multibeam echosounder, which is the ship's shallow-water (<500 m) system. It operates at nominal frequencies between 70 and 100 kHz with a total of 256 beams with angular dimensions of $1° \times 2°$. In greater depths, or where the acquisition of good-quality backscatter data was prioritised, the alternate deep-water system, the Kongsberg Maritime EM122, was used, operating with 288 beams per swath (angular dimensions are $1° \times 1°$) at a frequency of 12 kHz (Bohrmann et al., 2017). Onboard the *RV Polarstern*, bathymetric data were acquired with a Teledyne RESON Hydrosweep DS3 multibeam echosounder operating at nominal frequencies between 14 and 17 kHz and a variable number of beams according to water depth (Kasten, 2023). All bathymetric data were processed with the open-source software MB-System (Caress and Chayes, 2017), gridded to a resolution between 5 and 50 m, depending on data quality, and visualised and interpreted in Global Mapper 24.0 and ESRI ArcGIS® Pro. With the exception of Fig. 1a and b (South Pole Stereographic and World Transverse Mercator projection, respectively), all maps were produced in the UTM projection for zone 24 S, datum WGS84.

The Teledyne ATLAS PARASOUND P70 sub-bottom profiler is installed on both vessels and was used to acquire the sediment echosounder data for this study. The system was operated at two main frequency bands, a primary high frequency (PHF) between 18 and 20 kHz, and a secondary (parametric) low frequency (SLF) of ~4 kHz, the latter of which is used for seafloor stratigraphy. Sub-bottom profiler data were visualised and interpreted using SMT The Kingdom Suite v. 2019.

4. Results

4.1. Seafloor morphology – description and interpretation

The bathymetric data presented in this study show that KHTS is characterised by a variable seafloor morphology. The most distinct features are the trough basins of KHT, JT and AT within otherwise much shallower surrounding shelf regions (Fig. 2a). KHT is around 250 m deep in its northern parts, deepens to ~350 m toward the mid-shelf and shoals to around 300 m at the shelf edge. It thus shows a slightly reverse bed slope on the mid- and outer shelf, which is common for many cross-shelf troughs (cf. Graham et al., 2008; Rydningen et al., 2013; Ryan et al., 2016). Moreover, the water depth on the western side is generally deeper than on the eastern side of KHT (Fig. 1c), expressing a lateral asymmetry comparable to cross-profiles of glacial troughs around the Antarctic Peninsula and Iceland. Similar to those troughs, where asymmetric trough incisions have been related to preferential erosion of weaker bedrock/subglacial substrate on one side of the troughs (Evans et al., 2006; Spagnolo and Clark, 2009), the NE-SW orientation of central KHT is parallel to a fault inferred by Graham et al. (2008), and therefore suggests similar formation mechanisms for KHTS.

Several basins are overdeepened with respect to the remaining trough basin and are between 1 and 5 km long, up to 1.5 km wide, and up to 380 m deep (Fig. 2a). These basins, with their respective sedimentary infill, have previously been interpreted as moat-drift systems, developing from a dynamic regime of bottom-currents (Lešić et al., 2024). The largest moat is located at the confluence zone between KHT

and JT, but several smaller ones are clustered along KHT's western flank (Fig. 2b). JT and AT, on the other hand, have their deepest parts close to the confluence zone with KHT and shallow towards the coast, ranging in depth from 350 to 380 m.

Bathymetric shoals often appear as larger plateau areas, especially around the trough flanks. They have generally rugged surfaces (Figs. 2c, d; 3b), and, based on this and their widespread occurrence, are interpreted as outcropping bedrock. This is also supported by the sub-bottom profiler data (see section 4.2 below). Many of these bedrock surfaces host a number of small, elongate, more or less parallel, ridge-like features, that, on the inner and mid-shelf, are around 500 m long and 5–10 m high. On the outer shelf, these features are much longer with lengths between 2 and 4 km (Fig. 2b and 3b) and appear to be, at least partially, associated with the softer sediment sequences in the trough basin. Their width of ~70 m is relatively uniform across the entire trough system and they usually occur in groups (Fig. 2b). The ridges are generally E-W orientated in JT (Fig. 2b and c) and mostly NE-SW orientated in KHT (Fig. 2b and 3b). Such characteristically aligned bedrock has previously been classified as streamlined seafloor (Dowdeswell et al., 2016a) or ice-moulded bedrock (Ó Cofaigh et al., 2005), and is in accordance with similar observations around South Georgia (Graham et al., 2008, 2017; Hodgson et al., 2014a; Lešić et al., 2022). Individual lineations in KHTS (Fig. 2b and c) are interpreted as streamlined bedrock and crag-and-tails on the inner and mid-shelf (cf. Ó Cofaigh et al., 2005; Graham et al., 2008, 2017), forming when grounded ice modifies the pre-existing substrate, and deposits material in the lee of some erosion-resistant bedrock obstacles (e.g. MacLean et al., 2016). Although characteristic sedimentary glacial lineations appear to be absent in KHTS, the appearance of the linear features on the outer shelf and their association with the smooth sedimentary surface of the trough basin are in accordance with an interpretation as glacial lineations (e.g. Tulaczyk et al., 2001; Spagnolo et al., 2014). For simplicity, unless specifically stated, streamlined seafloor, crag-and-tails as well as the outer-shelf lineations will be summarised and referred to as "glacial lineations" from this point onwards.

Several semi-arcuate ridges on the mid- and outer shelf are orientated roughly perpendicular to the main trough axis and occur in two clusters, one on the eastern trough flank of KHT, and one in the main trough basin close to the shelf edge (Figs. 2b; 3d,e). The ridges along KHT are 500–700 m wide, 5–10 m high, and have a crest-to-crest spacing of ~1000 m. Close to the shelf edge the ridges are 6–8 m high and around 400 m wide, although one feature is 16 m high and 1 km wide. Because the ridges extend beyond the coverage of our dataset, their length cannot be determined accurately, but they appear to be longer than 2 km. Note that length in this context refers to the cross-trough extent, while width describes the along-trough extent. Because the ridges are similar to morainal ridges observed in Drygalski Trough (Lešić et al., 2022), and partially coincide with the location of previously documented ice-marginal moraines (eastern KHT flank; Graham et al., 2008), they are interpreted as recessional moraines, forming through intermittent still-stands of an overall retreating ice margin (e.g. Dowdeswell et al., 2008b; Ottesen and Dowdeswell, 2009). Although distances between individual ridges seem larger than normally postulated for annual push moraines (50 to a few hundred m), their regular spacing is indicative of regular, maybe even annual, formation (Dowdeswell et al., 2016a). This is also in accordance with their generally small size, which is likely related to shorter still-stands and/or limited sediment transport to the grounding line from a comparatively small ice cap. The larger feature may accordingly represent a longer period of ice margin stagnation, possibly due to a climatically colder or wetter period lasting several years or even decades (cf. Ottesen and Dowdeswell, 2009; Dowdeswell et al., 2016a).

In addition to the smaller, well-defined moraines, we identify four large bathymetric highs, BH1 to BH4 (Fig. 2a,b). BH1 is located in JTS, is orientated roughly ESE-WNW, and was documented to separate JT from AT in section 2 (Fig. 1c). Its surface is rugged and, in parts, intensely
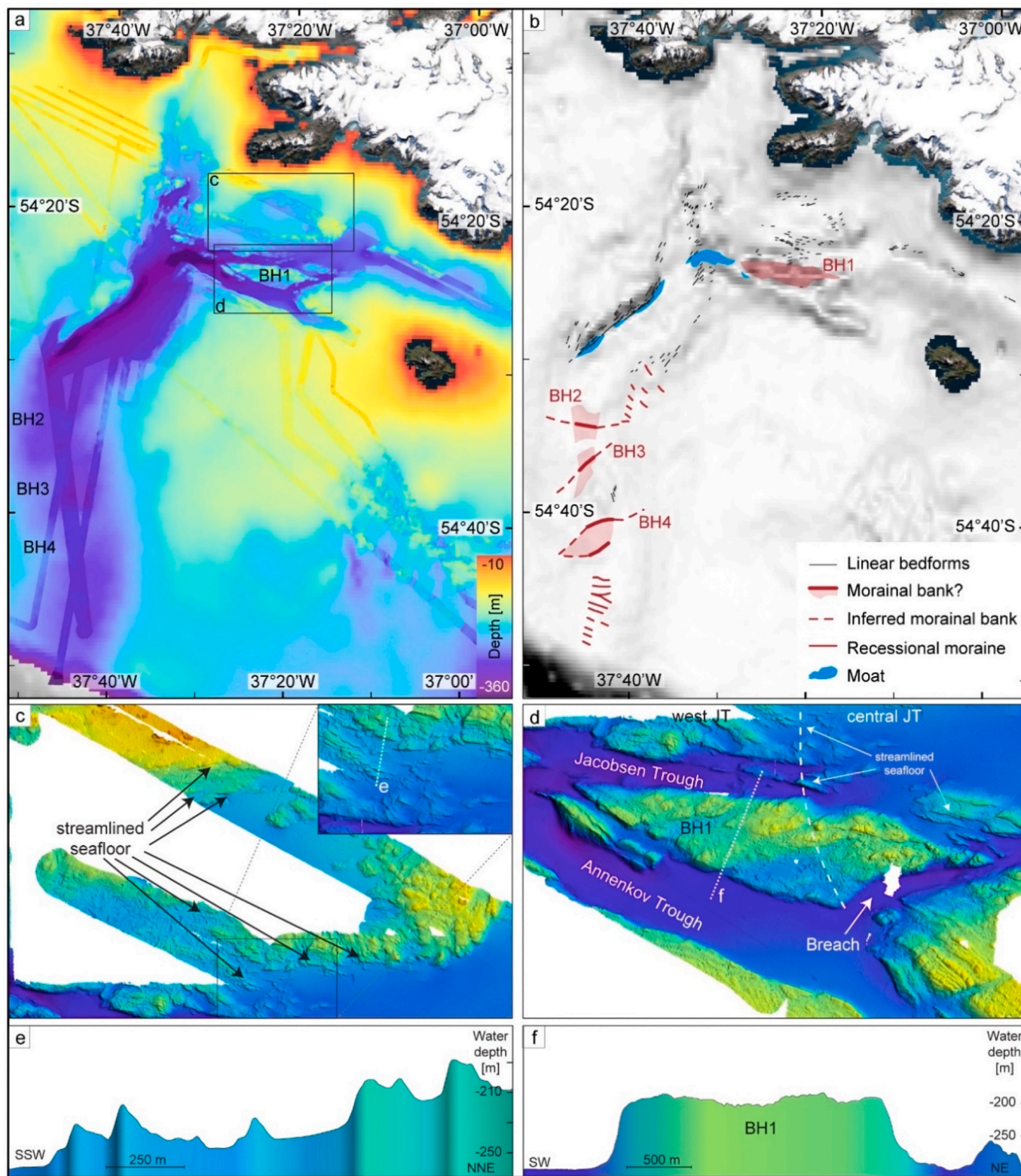
Fig. 2. a) Overview of the bathymetry used for this study as well as some landform examples from JTS. Background is a composite of the General Bathymetric Chart of the Oceans (GEBCO Compilation Group, 2023) with a grid-spacing of 500 m and a cropped version of the modelled bathymetry (grid spacing = 100 m) provided by Hogg et al. (2017). b) Map of the geomorphological landforms and their distribution within KHTS. c) Streamlined landforms in JTS with a zoom-in showing the more detailed crag-and-tail-like features, as well as the location of the cross profile shown in e). d) Close-up of the bathymetric high, BH1, in JTS, with the white dashed lines indicating the location of the cross-profile shown in f). e), f) Cross-profiles across streamlined seafloor and BH1 in JTS, respectively.
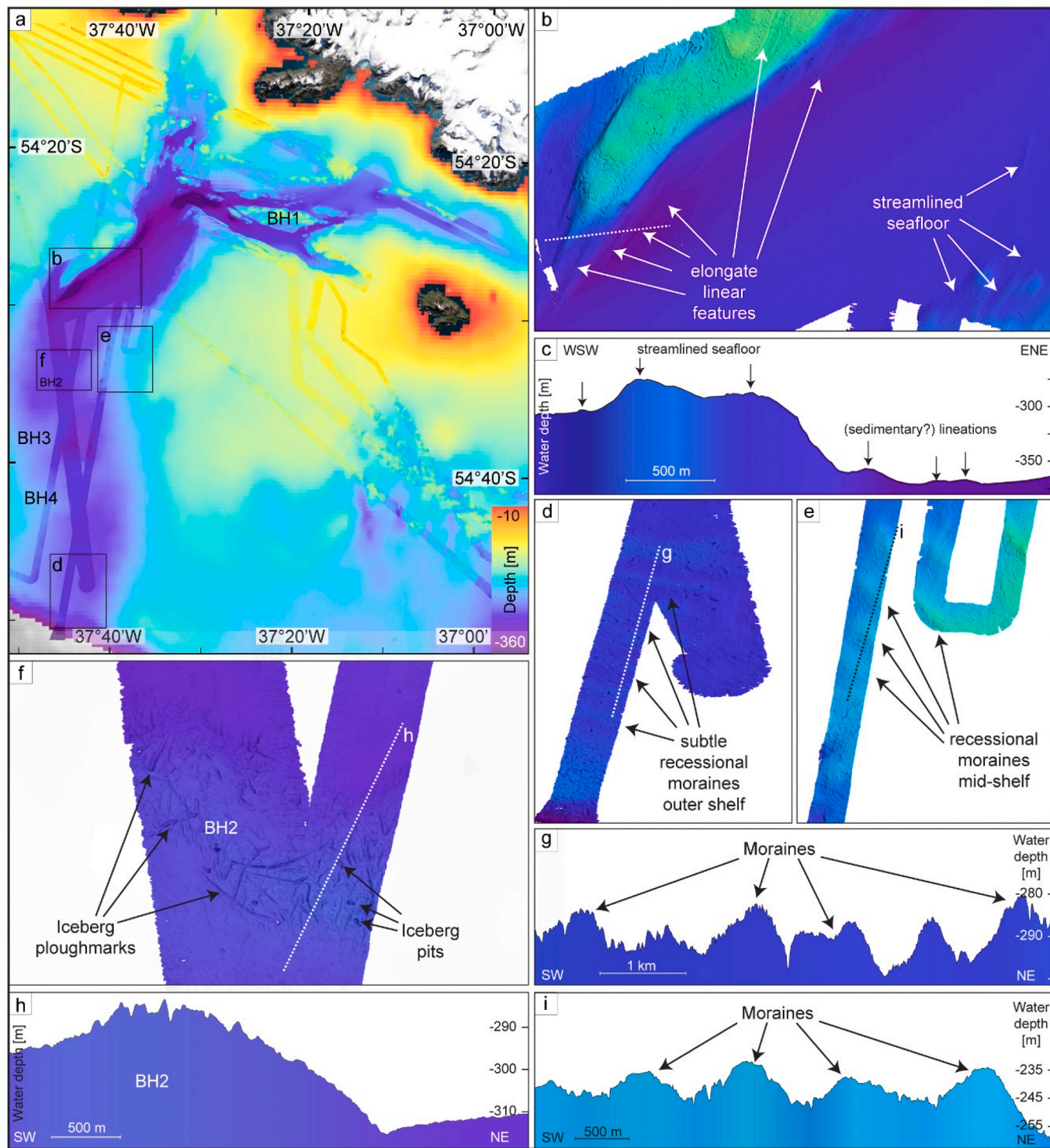
Fig. 3. Examples of the landforms observed in the bathymetric data from KHT. a) Overview map of the bathymetry used in this study. Black rectangles show the locations of individual sub-panels. b) Detail image of streamlined seafloor and elongate lineations in central KHT, with the white dashed line illustrating the position of the cross-profile shown in c). c) Cross-profile across the streamlined features in b). d), e) Recessional moraines observed on the outer and on the mid-shelf in KHT, respectively. White dashed line in g and black dashed line in e mark the locations of the cross-profiles shown in sub-panels g) and i), respectively. f) Close-up of bathymetric high BH2 on the mid-shelf in KHT. Note the obvious iceberg ploughmarks and pits on the surface. White dashed line marks the position of the cross-profile shown in sub-panel h). g), h), i) Cross-profiles across the recessional moraines in d), across BH2, and across the recessional moraines in sub-panel e), respectively.
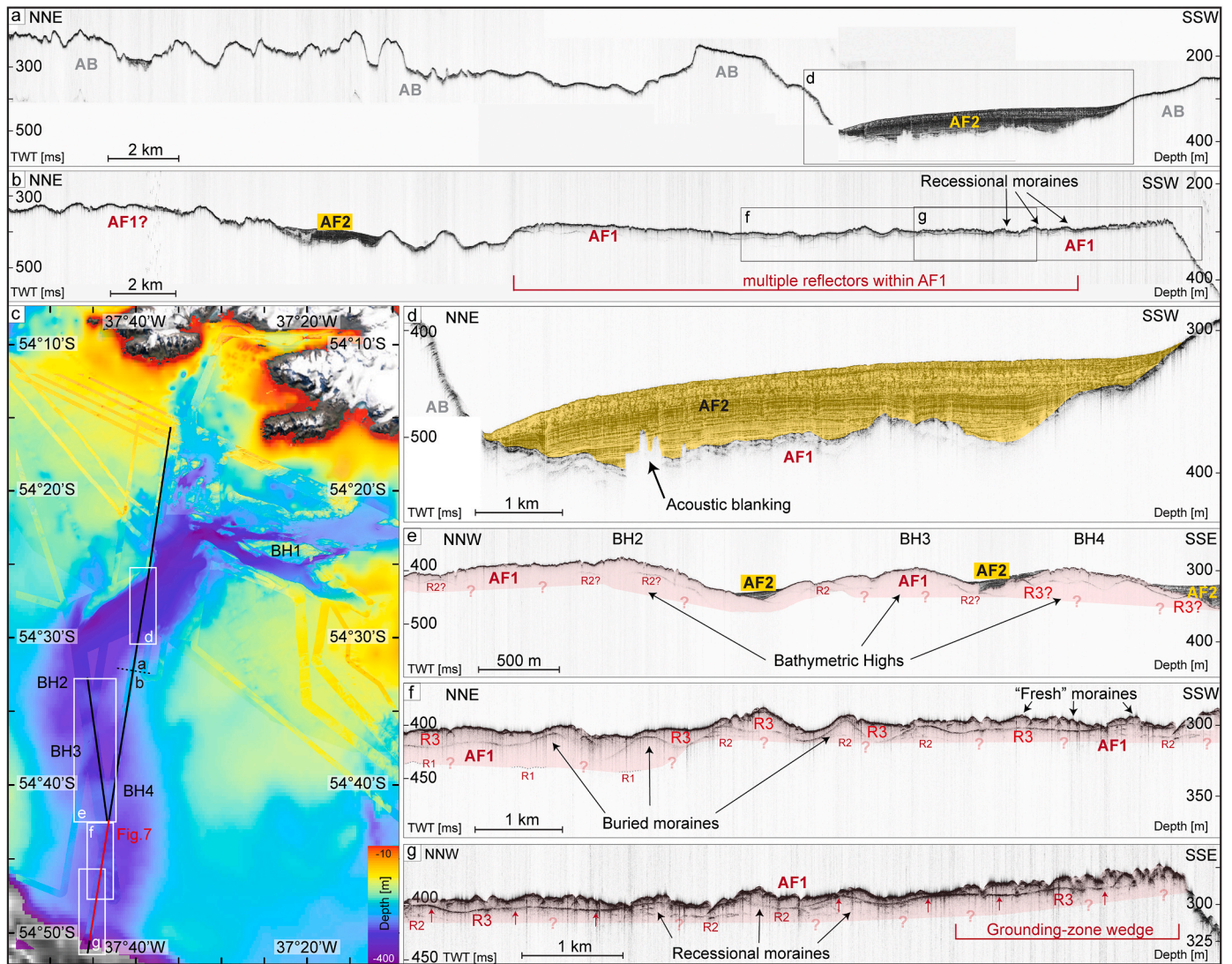
Fig. 4. Examples of the sub-bottom profiler data across KHT. a, b) Northern and southern part, respectively, of a NNE-SSW profile across the shelf. The distribution of the identified acoustic facies, AB, AF1, and AF2, is indicated. Black rectangles show the extent of sub-panels d, f and g. c) Bathymetric map of KHTS showing the location of the two illustrated sub-bottom profiles. The four bathymetric highs, BH1–BH4, are labelled. Red line shows position of the profile displayed in Fig. 7. d) Sub-bottom excerpt from the main trough basin of KHT with the thick sequences of AF2. Note the diffuse top reflector of AB in the NNE, and the acoustic blanking in the subsurface. e-g) Sub-bottom excerpts of AF1 on the mid- and outer shelf with the reflectors, R1-R3, labelled. e) NNW-SSE profile across three of the bathymetric highs, BH2–BH4, interpreted to be morainal banks. Small deposits of AF2 are labelled and some internal reflectors of AF1 are indicated. f) Distribution of AF1 with respect to fresh and buried moraines on the outer shelf. g) Sub-bottom data from the outermost shelf clearly show the reflectors R2 and R3 within AF1. Recessional moraines occur at the seafloor but also in the subsurface. AF2 is absent. Note that, due to the patchy occurrence of R1, it is unclear how far AF1 penetrates into the subsurface and its true extent may, in places, be much smaller. Question marks demarcate this uncertainty.

furrowed (Fig. 3c). It is up to 130 m high, up to 2.7 km wide, and about 13 km long. Geometrically, BH1 seems to be symmetric, with equally steep (~15° incline) proximal and distal flanks (Fig. 2f). A notable, straight, channel-like feature characterised by a very smooth surface breaches BH1 in a roughly NE-SW orientation, and eventually connects into AT (Fig. 2d). While the overall orientation of BH1 is parallel to an inferred extension of the Cooper Bay Shear Zone (CBSZ, Fig. 1b; Dalziel et al., 2021; also referred to as the Cooper Bay or Cumberland Bay Dislocation Zone; Macdonald and Storey, 1987; Graham et al., 2008), which marks a large tectonic boundary on the island, the breach coincides with the location of an additional fault inferred by Graham et al. (2008). BH2, BH3, and BH4 are more subtle, trough-transverse bathymetric highs that occur consecutively more seaward in KHT (Fig. 2a and b). Geometry and dimensions of these highs differ significantly from the previously described moraines, because they are both higher (16–18 m) and much wider, with a minimum along-trough width of ~3–7 km.

Since only parts of these features are covered by the hydroacoustic data, their geometry and exact dimensions are difficult to assess. Profiles across BH2, which is best resolved in our data, seem to indicate asymmetry, with a steeper proximal and a flatter distal side (Fig. 3f–h). It is unclear how exactly BH1–BH4 formed, although an interpretation as bedrock highs or morainal features seems reasonable. We distinguish between BH1 and the other three ridges, because the rugged appearance and steeper flanks of the former seem to suggest that BH1 represents a large bedrock high, which was partially covered by softer glacial deposits, as indicated by the presence of iceberg furrows. In contrast, BH2 to BH4 are much more subtle and therefore probably formed as purely ice-marginal features. Since BH2 was previously interpreted as a morainal bank (Graham et al., 2008), we also favour this interpretation for BH3 and BH4. This is further discussed in section 5.4.1 below.

Those parts of KHTS located in water depths below 310 m are characterised by smooth seafloor, probably imparted by locally

enhanced sediment accumulation (see also Lešić et al., 2024), and contrast the rugged surfaces of some of the landforms documented above (cf. Fig. 2a). Indeed, many of the shallower areas, including the moraines and bathymetric highs, appear to be heavily dissected, and exhibit a wide array of, mostly chaotically orientated, partially cross-cutting, ridges and furrows (e.g. Fig. 3f). These are highly variable in length, width, and height/depth and are often accompanied by small, up to 10-m-deep, circular to angular depressions with a diameter between 30 and 150 m (Fig. 3f). The chaotic orientation and the variable dimensions of the furrows are common characteristics of iceberg ploughmarks (cf. e.g. Barnes and Lien, 1988; Dowdeswell et al., 2010; Arndt and Forwick, 2016). Since icebergs with keel depths up to ~600 m have been documented from Antarctica (Dowdeswell and Bamber, 2007), water depths <310 m are a likely target for iceberg scouring in South Georgia, and we thus interpret the furrows as iceberg plough-marks. Although the associated depressions could represent pockmarks that have been documented in the subsurface of South Georgia trough sediments and formed through fluid seepage (Römer et al., 2014; Geprägs et al., 2016), we would mainly expect pockmarks to appear in the deeper trough basins amidst thicker sediment sequences. Instead, the close connection between the iceberg ploughmarks and the depressions suggests that the latter represent iceberg pits, marking the grounding or lift-off zones of the respective icebergs.

4.2. Seafloor stratigraphy

4.2.1. Acoustic facies - description

Sub-bottom profiler data reveal a total of two acoustic facies, AF1 and AF2. Although difficult to discern, as the signal is often obscured by overlying stratigraphic sequences, we additionally identify the acoustic basement, AB, in some places (Fig. 4). AB is acoustically almost impenetrable, with very few discontinuous, semi-opaque internal reflections. AB's top reflector, where imaged, coincides with the seabed in some areas, where it has an opaque and irregular, hummocky appearance. In steep terrain, the reflector is characterised by a diffuse appearance. AB crops out locally, specifically in central and west JT, as well as in northern KHT (Figs. 4, 5). Because AB represents the acoustic basement, we would expect it to be present everywhere in KHTS and to represent the oldest material. Nevertheless, AB's top reflector is only resolved locally, as it is often subject to acoustic blanking or hampered signal penetration through the overlying stratigraphic sequences. Along bathymetric slopes the irregular top reflector becomes more diffuse and is partially composed of a series of overlapping diffraction hyperbolae (Fig. 4d).

AF1 is acoustically semi-transparent at the surface and increasingly transparent with depth (Fig. 4e–g). It appears internally homogeneous, with generally scattered and chaotic, discontinuous reflections of vertically decreasing amplitude. It is characterised, however, by several distinct reflectors, marked R1-R3 in Fig. 4e–g. The lowermost visible reflector, R1, is highly discontinuous and is present only in a few locations on the outer shelf (Fig. 4f). Because of attenuated signal strength with depth, it is impossible to say whether R1 marks the top reflector of AB, and, thus, the bottom reflector of AF1, or whether it represents a facies-internal reflector. R2, where visible, is similarly discontinuous but generally more defined (Fig. 4e–g). In contrast, R3 is continuous across large areas of the continental shelf, and takes on a wavy appearance (Fig. 4e–g). It extends all the way to the shelf edge where it becomes increasingly flat (Fig. 4g). Some discontinuous, chaotic reflections occur between R3 and the seabed, but they are hard to distinguish. Together, they might represent a fourth internal reflector, R4, but this is impossible to ascertain. Especially in the outer-shelf regions, the top of AF1 is hummocky with a chaotic, mostly opaque appearance. Because it generally seems to coincide with the strong and opaque, rather thick, seabed reflector, this makes it difficult to discern the actual seabed and the top of AF1 from a potentially present, thin sediment cover. AF1 seems to mainly occur on the outer shelf in KHT (Fig. 4), although thick

sediment sequences and acoustic blanking could obliterate any appearances of AF1. Acoustic blanking is indeed common on the inner and mid-shelf, where it was attributed to the presence of free methane gas in the thick trough deposits (Römer et al., 2014; Geprägs et al., 2016). In these areas, AF1 may occasionally be present as a thin veneer on top of outcropping AB or beneath AF2 (Fig. 5b), but due to its similarity to AB, the two facies are difficult to differentiate in these locations. AF1 occasionally crops out at the seafloor, where it appears to form the previously described moraine ridges as well as the morainal banks BH2–BH4 (Fig. 4e–g).

AF2 is characterised by acoustic stratification, imparted by generally well-defined, parallel, internal reflectors of variable amplitude (Figs. 4d and 5), and has been described in detail by Lešić et al. (2024). On the basis of three distinct and continuous internal reflectors, AF2 was subdivided into four sub-units, A (oldest), B, C, and D (youngest). Unit AF2-A is seen to directly overlie AF1 in several locations on the mid- and outer shelf (example in Figs. 4d and 5b), but is not resolved in the Jacobsen-Newark Tributary, although this may be due to acoustic blanking (Fig. 5). AF2 was sampled by two gravity cores and consists of silty mud, with frequent diatom layers intercalated into Unit AF2-A (Lešić et al., 2024). AF2 conformably overlies stratigraphically older facies in KHTS, and is commonly confined to the bathymetric basins (Figs. 4a,b,d,e; 5b). It is present everywhere on the inner and mid-shelf of KHTS, but is absent on the outer shelf.

Lešić et al. (2024) obtained radiocarbon dates from the upper parts of AF2-A in two locations, one in KHT close to the confluence zone (core PS133/2_17–13), and one in central JT (core GeoB22058-1). Two ages from each location were used to provide relative age validation and to determine linear sedimentation rates (Lešić et al., 2024). The construction of an age model and an age of 10.2 cal ka BP revealed that the upper 388 cm of AF2-A were deposited over a time period of ~2.6 ka at assumed linear rates between 92 and 211 cm ka^{-1} in central JT, whereas the upper 582 cm in KHT were deposited after 9 ka BP at rates between 359 and 837 cm ka^{-1} (Lešić, 2024). Since both gravity cores only sampled the upper fraction of AF2-A, the two ages derive from a relatively shallow position within the unit (Lešić et al., 2024). Units AF2-B, AF2-C and AF2-D were determined to be of mid- to late Holocene age (Lešić et al., 2024; Lešić, 2024) and are hence considered to be outside the scope of this paper.

4.2.2. Acoustic facies - interpretation

Based on its acoustic character, AB seems to consist of a stiff or hard material through which the acoustic signal cannot travel easily. It could hence represent bedrock or glacial till (cf. e.g. Forwick et al., 2010; Forwick and Vorren, 2011; Streuff et al., 2017b). Because AB is difficult to distinguish where it underlies younger sequences, there is insufficient evidence for an unequivocal interpretation. But based on the fact that, in contrast to AF1, it is acoustically almost completely impenetrable, and because outcrops of AB often coincide with the position of the previously described bathymetric shoals, we consider an interpretation as bedrock more likely. This is supported by its diffuse character particularly on bathymetric slopes and its irregular top reflector (e.g. Ó Cofaigh et al., 2001, 2002; Evans et al., 2004). We cannot, however, exclude the possibility that AB represents bedrock in some and glacial till in other places, or that it comprises bedrock at the bottom and a thin cover of glacial till at the top.

The acoustic character of AF1 is not only similar to that of AB, but also to till observed in other glaciated regions (e.g. Pine Island Bay and the Antarctic Peninsula; Ó Cofaigh et al., 2005; Evans et al., 2006). Indeed, acoustically transparent till from the Antarctic shelf is associated with the same continuous, opaque, sometimes wavy reflectors as those observed within AF1 (Ó Cofaigh et al., 2002). Furthermore, similar reflectors to R1-R3 have previously been identified as the top of buried ice-marginal moraines or grounding-zone wedges (Ó Cofaigh et al., 2005) and as glacial erosional surfaces (Ó Cofaigh et al., 2004). Tills with a nearly identical acoustic character as the one in KHTS have
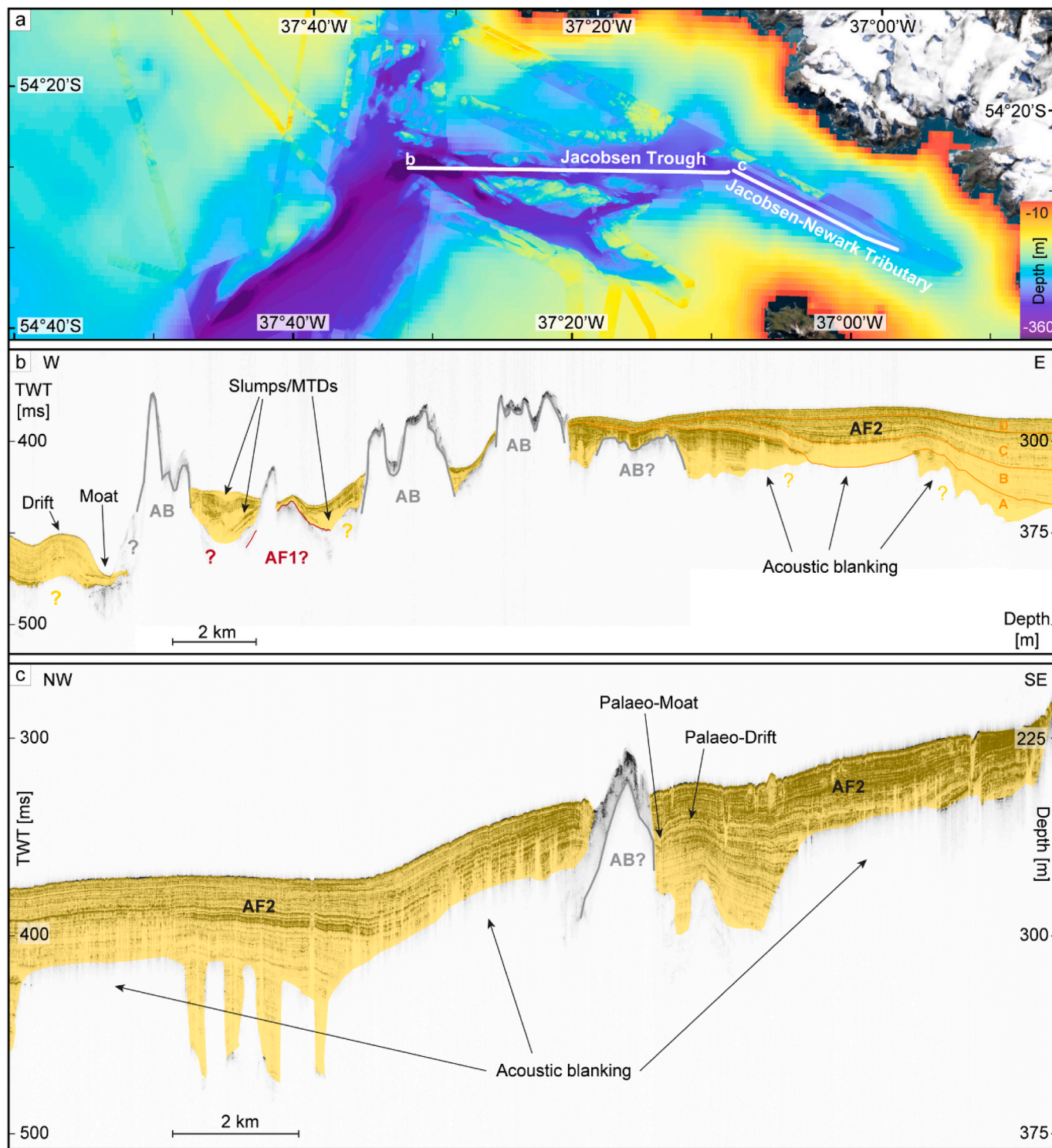
Fig. 5. Examples of sub-bottom profiler data through the Jacobsen Trough System (JTS). a) Bathymetric map of JTS with the location of the sub-bottom profiles shown in sub-panels b and c. b) Sub-bottom profile through Jacobsen Trough with AB cropping out at several locations. AF1 may be locally present, whereas (sub-units A-D of) AF2 represent the Holocene trough-fill sequences (Lešić et al., 2024). Near bedrock highs AF2 is disturbed and includes signs of slumps and/or mass-transport deposits (MTDs). Note acoustic blanking in the subsurface, partially obscuring the acoustic signal. A distinct-moat-drift system has developed around a bedrock high in the confluence zone. c) Sub-bottom profile through the Jacobsen-Newark Tributary. Acoustic blanking partially obscures the acoustic signal. A former moat-drift system can be seen within AF2 in the subsurface of the Jacobsen-Newark Bay.

actually been interpreted as stacked till sequences before (Ó Cofaigh et al., 2005), and we accordingly interpret AF1 with its internal reflectors to represent a sequence of at least three separate till generations, formed during repeated advance/retreat cycles of the SGIC. This is discussed further in section 5.3.2 below.

AF2 was interpreted as basin-fill sediment, deposited from mainly hemipelagic sedimentation (Lešić et al., 2024). The composition of the silty mud in combination with South Georgia's isolated position in the Southern Ocean implicates run-off from the island to be the main contributor to marine sedimentation. The exception are the

concentrated diatom layers intercalated into the terrigenous muds of Unit AF2-A, which were interpreted as the product of regular phytoplankton blooms (Lešić et al., 2024). The acoustic stratification of AF2 was suggested to represent periodic changes in the degree of primary productivity, rainout from meltwater plumes, iceberg rafting and occasional gravity-flows, whereas the distinct unit boundary reflectors provide evidence for several trough-wide changes in depositional environments.

5. Discussion – glacial history of KHTS

5.1. Trough origin

KHTS was interpreted as one of several cross-shelf troughs around South Georgia, formed from glacial erosion (Graham et al., 2008, 2017). The presence of (sub-)glacial till (AF1) deposited as, presumably, the first sedimentary sequence on top of the acoustic basement, and the occurrence of glacial landforms observed in our acoustic data, provide evidence that KHT indeed hosted grounded ice that likely carved out the trough valley over the course of one or more glaciations. The N–S orientation, its slightly retrograde bed slope along the outer shelf part of KHT and its lateral asymmetry are not only in accordance with other such troughs spreading roughly radially from the island (Graham et al., 2008), but also with cross-shelf troughs on other polar continental margins (cf. Evans et al., 2006; Graham et al., 2009; Spagnolo and Clark, 2009; Rydningen et al., 2013; Ryan et al., 2016), thus further strengthening the postulated glacial origin.

In contrast to the N–S orientation of KHT, the E-W, and de facto, *along*-shelf orientation of JTS is at odds with formation as a regular cross-shelf trough. Nonetheless, the presence and orientation of the parallel, streamlined glacial landforms in JTS show that ice must have also been grounded in this trough, flowing from generally (north)east to (south)west (Fig. 2b and c; see also Fig. 7 below). Although it is unclear why an ice stream or trunk glacier would have followed an along-shelf direction before joining KHT and changing to a cross-shelf direction, it is likely that ice-flow was directed along the Cooper Bay Shear Zone, thus facilitating trough formation in an E-W direction (Fig. 1b; cf., e.g. Graham et al., 2008). This is supported by the relatively steep trough flanks (especially along BH1; Fig. 2d), the sharp trough turn at the confluence with KHT, as well as a palaeo-ice flow direction that does not follow the most direct pathway offshore, because all of these are characteristics also associated with troughs in West Antarctica, where grounded ice sheets followed "the structural grain of the underlying bedrock" (Wellner et al., 2001). Although one might argue that there is no indication for (sub-)glacial sediment in JTS since neither AB nor AF1 can be clearly observed in its sub-surface (cf. Fig. 5), the presence of streamlined landforms and the connection to a series of glacier-fed tributaries provide clear evidence for the contribution of streaming ice also to the formation of this trough.

5.2. Streaming ice

Glacial landforms are present in JTS and KHT and therefore provide unequivocal evidence for grounded ice on the southwestern South Georgia continental shelf during a peak glaciation. Glacial lineations in KHTS indicate periods of streaming ice, with palaeo-ice flow from (north)east to west in JTS, but from north to south in KHT. As both KHT and JTS have a number of marine-terminating glaciers at their heads, it is probable that several ice streams were involved in the establishment of an ice stream and, thus, trough formation (Fig. 6). We hence hypothesise that an extended Briggs Glacier, likely as the main trunk glacier, drained the SGIC from east to west through King Haakon Bay, before being joined by the N–S draining Pride and Peters Glaciers just west of the sill/moraine (Fig. 6). The first appearance of short and crude streamlined bedforms just north of the KHT-JTS confluence zone (Fig. 6) suggests not only a change to a more NE-SW-orientated ice flow

direction, but also the onset of ice streaming on the inner shelf (cf. Wellner et al., 2001; Ó Cofaigh et al., 2005). Similarly, the distribution of streamlined bedforms in JTS implies that a palaeo-trunk glacier, presumably composed of Christophersen, Eclipse and Bary Glaciers, drained the SGIC in an E-W direction through Jacobsen Bight, being joined by several N–S-draining tributaries on its way through JTS (Fig. 6). Together, these glaciers probably exploited the above-postulated tectonic weakness along the CBSZ, thus contributing to the further evolution of the trough system. Just west of the confluence zone with KHT the Briggs and Christophersen trunk glaciers would have merged, developing into a composite ice stream draining the SGIC all the way to the shelf edge (Fig. 6).

The linear glacial features in KHTS evolve from crudely streamlined seafloor and shorter crag-and-tails on the inner and mid-shelf to more elongate glacial lineations towards the outer shelf (cf. Figs. 2a,b, 3d). Since here their elongation ratios often exceed 10:1, they are similar to glacial lineations observed around West Antarctica and the Antarctic Peninsula, and may be considered indicative either of fast-flowing ice or of a changing bed substrate (Stokes and Clark, 1999; Wellner et al., 2001; Graham et al., 2009). Indeed, since some of the glacial lineations in outer KHT occur in the, presumably softer, sediment sequences of the trough basin, and because the acoustically transparent facies above R3 (Fig. 4e–g) may comprise soft, water-saturated, weak deformation till (see also section 5.3.3 below), the ice sheet substrate might already have been softer than the rugged bedrock on the inner and mid-shelf during the formation of the attenuated glacial lineations. Till sequences such as the one overlying R3 have also been related to glacial lineations around Antarctica (e.g. Licht et al., 1999; Shipp et al., 1999; Wellner et al., 2001; Evans et al., 2005) and have previously been suggested to foster their formation as a result of facilitated ice movement (Ó Cofaigh et al., 2005; King et al., 2009). Because the characteristics of the glacial lineations in outer KHT are broadly comparable to those of mega-scale glacial lineations around Antarctica (increased elongation ratios, parallel alignment, close proximity), they might further provide evidence for warm-based ice in outer KHT at the time of their formation (cf. Klages et al., 2015).

5.3. Maximum ice extent

5.3.1. Evidence from glacial landforms

A terminal moraine marking maximum ice extent is lacking in KHTS, but the continental shelf edge slopes upwards for the outermost 2.6 km, thus generating a ~20 m-high, likely sedimentary, "wedge" with a flatter (0.4°) proximal and a steeper distal slope, i. e. the uppermost portion of the continental slope (5.6°, Fig. 4g). Dimensions are at the lower end of the spectrum of smaller grounding-zone wedges (GZWs) in the Northern Hemisphere and the overall morphology appears similar to a GZW documented from the shelf break off Melville Bay in NW Greenland (#45 in Batchelor and Dowdeswell, 2015). This suggests that a GZW is present at the mouth of KHTS on the southwestern South Georgia shelf break (cf. Graham et al., 2008). As these large sedimentary depocentres form along the grounding lines of ice streams (Batchelor and Dowdeswell, 2015), we consider this evidence that the SGIC extended all the way to the shelf break also in KHTS. This is supported by the presence of both subglacial till and recessional moraines up to close to the shelf edge, and is also in accordance with previous studies that suggested the shelf edge to be the position of maximum ice extent during the LLGM (Clapperton et al., 1989; Graham et al., 2008, 2017; Barlow et al., 2016; Lešić et al., 2022). Interestingly, an outward bulge, associated with progradation of the continental slope as a result of glacigenic sediment input, or a trough-mouth fan, both often observed near previously glaciated shelf edges (cf. Laberg and Vorren, 1995; Taylor et al., 2002; Evans et al., 2006; Dowdeswell et al., 2008a; Lucchi et al., 2012; Ó Cofaigh et al., 2013; Camerlenghi et al., 2016), appear to be absent or very weakly pronounced at the mouth of KHTS and may indicate reduced sediment supply to the grounding zone from a comparatively
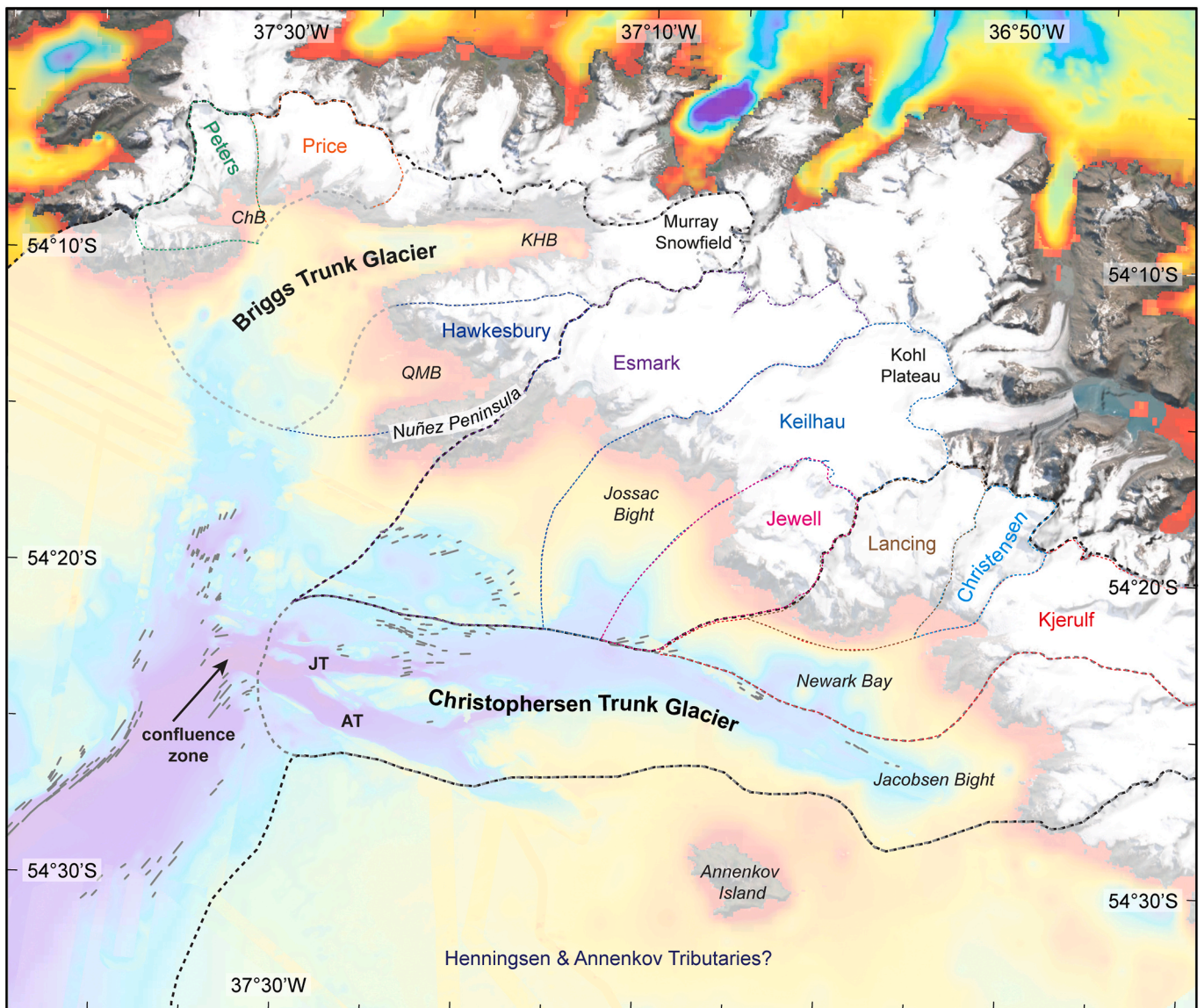
Fig. 6. Schematic ice drainage through KHTS during the LLGM with the juncture of two main trunk glaciers, Briggs and Christophersen Glaciers and respective tributaries, hypothesized. Streamlined landforms (dark grey lines) and most important locations are indicated, with CB = Cheapman Bay, KHB = King Haakon Bay, QMB = Queen Maud Bay, JT = Jacobsen Trough, and AT = Annenkov Trough. Place names are written in italic, glacial tributaries are labelled in colour and named after the respective source glacier. The confluence zone between JTS and KHT is arrowed. Please note that the conceptualisation is only intended to illustrate drainage pathways as reconstructed from the geomorphology - it cannot depict accurate ice extents or chronological information.

small ice cap. This is consistent with observations by Graham et al. (2008), who found a trough-mouth fan to be present in front of only one of the cross-shelf troughs around South Georgia.

All landforms in KHTS are generally well-preserved, meaning that they are still distinctly visible on the seafloor. As several studies suggest the LLGM (Marine Isotope Stage or MIS 2) to manifest the most recent extensive shelf glaciation in South Georgia (e.g. Clapperton et al., 1989; Graham et al., 2008; Barlow et al., 2016; Graham et al., 2017; Lešić et al., 2022), the most obvious conclusion would be that the landforms, or at least their majority, derive from this time. Indeed, none of the landforms show signs of having been modified after their formation, with the exception of the recessional moraine banks, which were merely subjected to intensive iceberg scouring. As a result, it seems unlikely that they were overridden by re-advancing ice since their formation, suggesting that they derive from the most recent shelf-wide glaciation in South Georgia. Moreover, assuming average post-glacial sedimentation rates from other previously glaciated continental margins (anywhere between ~0.01 and 350 cm ka^{-1}; Streuff et al. (2022)

and references therein) and an LLGM dating to some time between ~30 and ~18 ka BP (cf. Graham et al., 2017; Lešić et al., 2022), the low-relief glacial lineations and recessional moraine ridges would probably have been buried if they were older than the LLGM. In fact, radiocarbon dates from selected sites around the island implied rather high post-glacial sedimentation up to 837 cm ka^{-1} in central KHT (Lešić et al., 2024), between 10 and 53 cm ka^{-1} in the adjacent Drygalski Trough (excluding peak sedimentation during the Antarctic Cold Reversal; Fig. 1b; Lešić et al., 2022), and initially high (306 cm ka^{-1}) but increasingly lower sedimentation rates in Royal Bay Trough (RBT, Fig. 1b; Graham et al., 2017), making burial even more likely. An LLGM age for the landforms would also be in accordance with both Barlow et al. (2016) and Graham et al. (2017), who already attributed outer-shelf moraines to the LLGM, and would imply that the SGIC behaved similarly to ice masses around the Antarctic Peninsula and West Antarctica, where the LGM also forced shelf-wide extent (Dowdeswell et al., 2004; Evans et al., 2005; Larter et al., 2014; Ó Cofaigh et al., 2014). Lastly, an extensive LGM was also proposed for other sub-Antarctic islands (Hodgson et al., 2014b),

making maximum or at least close-to-maximum ice extent during the LLGM almost indisputable for South Georgia.

While, based on the above, we definitively ascribe KHTS landforms on the inner and mid-shelf to the LLGM, we cannot quite exclude the possibility of a pre-LLGM age for the GZW and the recessional moraines at the shelf edge. Firstly, the sub-bottom profiler data show no notable sediment cover on top of the glacial till (AF1), suggesting that post-glacial sedimentation rates could have been insufficient on the outer shelf to bury the landforms even over long periods of time. Indeed, rates presented above were from mid- or inner shelf positions and could be locally exaggerated by contourite drifts and bottom currents (Lešić et al., 2024). Secondly, the landforms may originally have been much larger, as GZWs and recessional moraines can attain thicknesses/heights of up to 200 m and tens of metres, respectively (Batchelor and Dowdeswell, 2015; Dowdeswell et al., 2016a). Accordingly, the majority of their relief may have been covered with only the uppermost 5 m preserved at the surface of the seafloor; unfortunately the sub-bottom profiler resolution is insufficient to evaluate this. Third, research on South Georgia has unearthed a long line of evidence apparently in favour of restricted LGM extents, with beach deposits underlying glacial till and showing clear signs of glacial modification (Sugden and Clapperton, 1977), the presence of proglacial lake sediments at 18.6 ka BP (Rosqvist et al., 1999) taken as evidence of a "within-fjord" LLGM (Bentley et al., 2007), peat deposits suggesting the presence of biological refugia, i.e. ice-free areas, during the last glacial (van der Putten and Verbruggen, 2005), and the combination of terrestrial and submarine moraine successions with cosmogenic nuclide dating used to postulate LGM ice to only reach the inner fjords (Hodgson et al., 2014a). Although these hypotheses have since been largely refuted, with strong evidence for shelf-edge or close-to-shelf-edge glaciation and some intermittent ice-free areas during the LLGM (Graham et al., 2008, 2017; Barlow et al., 2016; Barnes et al., 2016; Lešić et al., 2022), our data may indicate that the LLGM, albeit quite extensive, did not mark the maximum glaciation of the South Georgia continental shelf. This will be discussed throughout the following paragraphs.

5.3.2. Evidence from seafloor stratigraphy

As the first study to resolve sequences of stacked tills from the region, our sub-bottom profiler data provide evidence of repeated ice advances to the shelf edge. This is based on the presence of at least three separate generations of subglacial till (one above R1, one above R2, and at least one more above R3; see also section 4.2), which are schematically illustrated in Fig. 7. An interpretation of stacked tills, and hence separate till generations, was made on the basis of the presence of distinct internal reflectors and their similarity to such tills from the Antarctic Peninsula (Ó Cofaigh et al., 2005). It is also in accordance with similar findings from NE Greenland, where stacked acoustically transparent units, separated by (semi-)continuous opaque reflectors, were interpreted as till sequences (Ó Cofaigh et al., 2004). In both cases, sharp internal reflectors were interpreted as glacial erosional surfaces, which causes us to conclude that R3 also represents such a surface. We would further argue that R2 and R1 equally represent erosional surfaces related to glacial processes, as they are distinct enough to be picked up by the sub-bottom profiler in an otherwise acoustically transparent facies. Their much weaker appearance compared to R3 can be explained by general attenuation of the acoustic signal with depth. An interpretation of several till generations is further supported by the fact that AF1 forms moraines both in the subsurface as well as at the seafloor (cf. Fig. 4f and g). Although the latter could simply be related to draping, and thus maintenance, of the buried glacial landscape, R3 is present as a relatively flat reflector with superimposed moraines on the outer shelf (Fig. 7c), which immediately negates this possibility. One might further argue that the portion of AF1 above R3 (3rd generation till in Fig. 7d) could represent mass-flow deposits rather than glacial till. We consider this unlikely, however, as this part of AF1 occurs in a generally flat, low-accumulation terrain. Moreover, Ó Cofaigh et al. (2005a,b)

suggested a similar acoustic unit on the western Antarctic Peninsula to represent a sheet of (deformation) till. Such an interpretation is also supported by the presence of the much more elongated glacial lineations in outer KHT, and the absence of characteristically dipping reflectors and/or lenticular sediment bodies, which we would expect to see if, at least parts of AF1, were formed from mass flows.

Evidence of repeated ice advance to the shelf edge is in agreement with Clapperton et al. (1989) and Graham et al. (2017), who already suggested this from the presence of both truncated and well-preserved ice-sheet end moraines. However, while it may be true that the geomorphological data suggest only one episode of ice retreat and hence only one phase of deglaciation (Graham et al., 2017), the stacked tills in our sub-bottom profiler data do not necessarily paint the same picture. Indeed, assuming that an interpretation of the internal reflectors as erosive surfaces is correct and that erosive surfaces indicate only ice advance (the ubiquitous iceberg ploughmarks attest to calving as the main mechanism of retreat), the fact that all three reflectors extend from the mid-shelf all the way to (close to) the shelf edge would prove that ice advanced *and subsequently retreated to the mid-shelf* at least three times. The first advance would have been up to a few hundred metres from the shelf edge, depositing the first generation glacial till above R1 (Fig. 7b), the second would have been all the way to the shelf edge, leaving behind the second till generation above R2 (Fig. 7c), and the third (and probably last) advance would have deposited the third generation, which does not quite reach the shelf edge (~1 km away, Fig. 7d). Note that, because some of the reflectors are quite discontinuous or weakly pronounced in places, especially the extent of the first generation till may be exaggerated in Fig. 7. R1 is only clearly present up until the mid-shelf, so the first advance did not necessarily reach close to the shelf edge, or may have later been eroded. In contrast, despite poorer signal resolution close to the shelf break, R2 and R3 can both be traced at or close to the edge of the continental shelf, so we consider their illustration in Fig. 7 to be relatively reliable. It follows that R2 seems to surpass R3, and, therefore, that the second-to-last ice advance to the shelf edge - rather than the latest - was actually the most extensive. Besides the main reflectors R1-R3, some additional reflectors within AF1 may imply further till generations, but since the latter are highly discontinuous and only appear very locally, it is difficult to verify their origin as actual additional surfaces as opposed to potential geophysical artefacts.

5.3.3. Timing of maximum ice extent

Having established that the different sub-bottom reflectors within AF1 likely represent the bases of three different till units that all extend to (close to) the shelf edge, there remains the question of the timing of their formation. Although it has been postulated that the soft deformation till discovered in Marguerite Trough on the Antarctic Peninsula formed from the development of an ice stream only during the post-LGM deglaciation (Ó Cofaigh et al., 2005), we consider this unlikely for South Georgia, whose exposure to the ACC and the Westerlies would presumably have caused the ice cap to react quickly to warming temperatures. As a result, ice would likely have disintegrated rather rapidly, forced by both increased surface melt and pervasive subglacial melting (cf. studies in Greenland and Antarctica; e.g. Holland et al., 2008; Murray et al., 2010; Pritchard et al., 2012; Rignot et al., 2013). Indeed, a sustained ice stream in the trough during deglaciation seems improbable, particularly when considering that waterlain till in the adjacent Drygalski Trough (DT, Fig. 1b) implied the presence of a subglacial cavity and/or lightly grounded ice, probably causing ice to unground much earlier in the trough basin than on the surrounding shelf areas (Lešić et al., 2022). We therefore consider two plausible alternatives for the formation of stacked till sequences in KHTS: 1) the till generations formed over the course of several glacial events, with the first-generation glacial till (Fig. 7b) relating to a pre-LLGM event such as the Penultimate Glaciation (MIS 6), one of the colder sub-stages of MIS 5, or MIS 4. As the second generation till post-dates this first event, the till sequence above R2 (Fig. 7c) would have to be related to MIS 5b, MIS
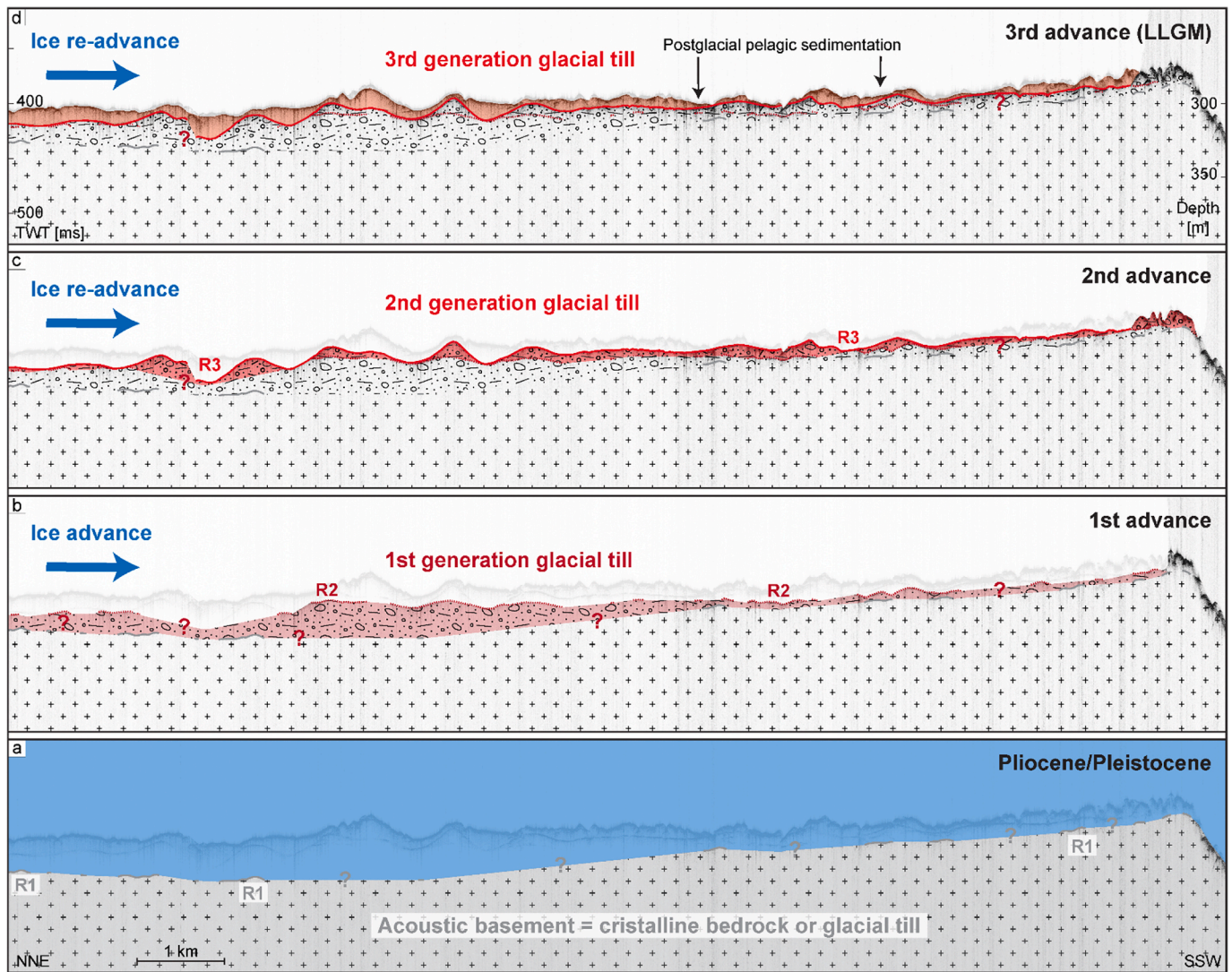
Fig. 7. Stacked till sequences and schematic illustration of the postulated glacial history of the King Haakon Trough System, exemplified by part of the sub-bottom profile displayed in Fig. 4b. For location check Fig. 4c. Note that, due to discontinuous reflectors within AF1, extents of individual till units may be different than illustrated here. Till generations may all originate from the same glacial event, e.g. LLGM, or could derive from separate glaciations. a) KHTS shelf prior to any glaciations (but after 6.4 Ma; cf. Graham et al., 2008). b) First ice advance, possibly during MIS 6 or one of the substages of MIS 5; deposition of the first generation of glacial till. c) Extensive ice re-advance during a later stage, possibly during a MIS 5 substage or MIS 3, surpasses the previous extent; formation of the second till generation. d) Another ice re-advance, likely during the LLGM (MIS 2) deposits a, slightly less extensive, third generation of subglacial till.

4, or to MIS 3, while the uppermost, third, till generation would have formed during ice advance related to the LLGM (MIS 2; Fig. 7d). 2) All three till generations originate from repeated advances during the LLGM, in which case the first generation till would have been deposited during an early LLGM-related ice cap expansion, followed by extensive retreat and then two renewed advance/retreat cycles.

Extensive Pleistocene glaciations have been shown in other sub-Antarctic regions, such as Patagonia, New Zealand, and the Kerguelen Islands, where ice extents were inferred to have been larger during MIS 3/4 than during the LGM (Darvill et al., 2015, 2016; Williams et al., 2015; Jomelli et al., 2018). Similar extensive glaciations have also been postulated for South Georgia (Hodgson et al., 2014b) and would support the first possibility, that the till generations derive from separate glaciations. Note, however, that these may all have taken place within the same glacial period, i.e. the Last Glacial (Wisconsinan/Weichselian Glaciation). In this case the second-generation glacial till would very likely date back to MIS 3, which, in turn, would show that MIS 3 was more extensive than the LLGM also on South Georgia. This would be in agreement with early work by Sugden and Clapperton (1977), who, on

the basis of geomorphological evidence from northeast South Georgia, claimed that "maximum ice cover predates at least one full glaciation". It would also explain why so many studies seemed to originally favour a restricted LGM extent for the SGIC. If the ice cap indeed behaved similar to ice masses on the other sub-Antarctic islands during the last glacial period, this would have a crucial implication for climate research: the sub-Antarctic islands and Patagonia, rather than being located north of the Polar Front, may actually have been situated on the same (southern) side as South Georgia. Indeed, several studies have put forth the idea that the positions of the Polar Front as well as the Westerlies varied over time. Glacial advances (retreats) in southern South America and New Zealand during and since the LGM have usually been connected to climatic cooling (warming), which, in fact, was generally associated with a northward (southward) migration not only of the core belt of the westerlies, but also of the main oceanic fronts in the region (e.g. Kaplan et al., 2008; Putnam et al., 2010, 2012; Kaplan et al., 2016). Despite the fact that records from South Georgia are still far from extensive, several studies have drawn similar conclusions (albeit post-LGM glacial re-advances connected to Southern Ocean cooling) for this region (e.g.

Bakke et al., 2021; Graham et al., 2017; van der Bilt et al., 2017; Berg et al., 2019), suggesting that a northward shift of the Polar Front during the last glaciation(s) is not at all unlikely. This shows, not only that past evolution of the islands may have been much more similar than previously thought, but also that the KHTS till generations relating to different glaciations is a real possibility.

In contrast, arguments could also be made for the second possibility, that the till generations related only to separate advance/retreat cycles during the LLGM. For instance, ice margin oscillations during the LGM are not unusual and have been documented for some portions of palaeo-ice sheets (e.g. Clayton et al., 1985; Ottesen et al., 2007; Thomas and Chiverrell, 2007). Moreover, many glaciers in sub-polar to temperate glacial regimes have been identified as surge-type (Post, 1969; Copland et al., 2003; Farnsworth et al., 2016), making it worthwhile to consider the possibility of ice front variability independent of regional climate. Both Briggs and Christophersen Glacier might have been prone to these cyclic phases of activity (advance) and quiescence (retreat; cf. Meier and Post, 1969), leading to potentially quite significant ice front re-advances. However, to our knowledge no glacier surges have been documented from anywhere around South Georgia, neither during, nor since the LGM, raising the question whether surges during the LGM were a likely possibility. Furthermore, since the SGIC was bound to be a spatially restricted ice cap with much less volume than any of the ice sheets postulated for North America, Svalbard and the Barents Sea, or Britain and Ireland, we would not expect that the SGIC had the capacity to reconfigure itself as dramatically. Accordingly, non-surge ice margin oscillations would presumably have occurred over much shorter distances. Nonetheless, the extent of the current data does not permit a definitive conclusion, for which deep records from drilling and seismic investigations would be necessary. Notwithstanding this, we maintain that the uppermost, i.e. 3rd, generation of glacial till (Fig. 7d) almost certainly derives from the LLGM, because this till sequence as well as unmodified glacial landforms extend until close to the shelf edge (see also section 5.2.1).

5.4. Deglaciation/ice retreat

5.4.1. Post-LLGM

Three large bathymetric highs (BH2–BH4) and two clusters of small trough-transverse moraine ridges were interpreted as recessional features deposited during overall ice retreat. Indeed, the recessional moraines probably indicate two phases in recession, where ice retreat was frequently interrupted by smaller still-stands and/or re-advances (cf. Ottesen and Dowdeswell, 2006). The larger-than-usual spacing for these regularly formed push moraines could be explained by generally faster retreat between periods of ice still-stand and/or by limited sediment delivery to the front of the receding ice sheet (cf. Dowdeswell et al., 2016a). In contrast, the bathymetric highs BH4, BH3, and BH2 probably indicate three periods where ice paused its retreat for longer periods of time. This is based on the much larger size and the subtle morphology. Although these highs do not give the impression of line-sourced sediment delivery (cf. Dowdeswell et al., 2016a) and are therefore more similar to GZWs than moraines, their comparatively small size and their apparent asymmetry, with a seemingly steeper proximal and a flatter distal side, are at odds with an interpretation as GZWs (cf. Batchelor and Dowdeswell, 2015). Furthermore, GZWs are typically associated with ice margins configured as ice shelves, and it would therefore be difficult to reconcile the presence of the distinct moraine cluster, more indicative of an ice cliff margin, with the immediately adjacent GZWs (Batchelor and Dowdeswell, 2015; Dowdeswell et al., 2016a). We accordingly maintain an interpretation as moraine banks for the bathymetric highs BH2 to BH4 (Graham et al., 2008) and suggest that, sensu Hunter et al. (1996), these features were formed as recessional features during three consecutive pauses in ice recession. This is also in accordance with similar mid-trough moraines on the NW continental shelf of South

Georgia, where one suggested possibility for their formation included marginal still-stands during overall deglaciation (Graham et al., 2008).

After the shelf areas became ice free, numerous deep-keeled icebergs in KHTS scoured the seabed, as attested to by the ubiquitous iceberg ploughmarks. Since South Georgia is located in the main trajectory of icebergs calved off the Antarctic Ice Sheet, the iceberg ploughmarks on the continental shelf might, in theory, derive from icebergs originating in Antarctica. This is unlikely, however, because the retrograde bedslope of KHTS would prevent the entry of such, much larger, icebergs into the trough. Accordingly, the numerous iceberg ploughmarks in KHTS not only provide evidence that ice recession of the SGIC happened predominantly by calving but also that calving must have happened relatively close to the grounding line. This is based on the fact that icebergs must have had keel depths exceeding 300 m to account for iceberg ploughmarks in water depths down to 310 m. Because this is unlikely if they were sourced from a seaward-thinning ice shelf, the presence of iceberg scours also supports our initial conclusion that the SGIC margin was configured as an ice cliff, rather than an ice shelf (cf. Dowdeswell et al., 2016a).

Following the discussion about several generations of glacial till and a potentially more extensive pre-LLGM glaciation in the previous section, it is possible, that while the moraine banks and recessional moraines on the mid-shelf almost definitively derive from the LLGM, the GZW and the recessional moraines close to the shelf edge actually predate the last glaciation. This possibility was already discussed on the basis of low sedimentation rates on the outer shelf in KHTS, but might become more likely in light of the sub-bottom profiler data. As the GZW at the shelf edge is predominantly composed of the 2nd generation till and the recessional moraines are found beyond the extent of the 3rd generation (Fig. 4e–g, 7c,d), it seems more logical to assume that both features were actually formed during the second-to-last glaciation, which does not necessarily relate to the LLGM (section 5.3.3).

Without additional radiocarbon dates, it is difficult to make reliable interpretations about the timing of deglaciation in KHTS. Extrapolation of the sedimentation rates, estimated on the basis of the radiocarbon dates obtained from the presumably first deglacial sediment sequence in KHTS, AF2-A (Lešić et al., 2024), would suggest that glacimarine sedimentation may have initiated as early as 31 ka BP, but before 12 ka BP (Lešić et al., 2024). Although these ages were discussed to be slightly unreliable, as the assumption of, locally quite variable, linear sedimentation rates likely over- or underestimates respective dates, this time frame is in line with findings from the adjacent Drygalski Trough to the east (Fig. 1b), where post-LLGM deglaciation and subsequent sedimentation could have started as early as 30 ka BP. Waterlain till from that trough dates to ~24.5 ka BP and indicates that (asynchronous) deglaciation was underway already prior to this time, with a subglacial cavity forming at the core site first. The subsequent destabilisation of the ice sheet from within created the necessary accommodation space for the ice-proximal sediments, before actual ice margin retreat from the surrounding shelf areas began just prior to 17.5 ka BP (Lešić et al., 2022). Glacial landforms in DT are similar to those in KHTS, which could indeed indicate a similar evolution during deglaciation after the LLGM. Moreover, post-glacial trough infill was postulated to have started around 17.9 ka BP in Royal Bay Trough in the northeast (Fig. 1b; Graham et al., 2017), implying that deglacial conditions may have been similar for the larger cross-shelf troughs around South Georgia. We previously mentioned that neither AF1 nor AB are resolved in the sub-bottom data of JT (Fig. 5) and discarded the possibility that this is related to an absence of glacial influence in the trough system. Although this apparent lack was likely caused by the very thick overlying sediment sequences placing AF1 and AB outside the signal penetration limits of the echosounder system, a second possibility could be the presence of a subglacial cavity below the LLGM ice cap, just as reconstructed for Drygalski Trough (Lešić et al., 2022). This would be feasible on the grounds of the pre-existence of a sufficiently deep basin (cf. Pine Island

Bay, Antarctic Peninsula; Kuhn et al., 2017) and the occurrence of streamlined seafloor only along the trough flanks. Although, we would, in that case, expect to find cavity-characteristic deposits in JT, the acoustic signature of the waterlain diamicton in Drygalski Trough (Lešić et al., 2022) is indeed similar to the acoustic stratification of AF2-A in KHTS and may suggest that such deposits are also present in JT and KHT. Furthermore, the cores sampling AF2-A were almost certainly too short to recover such sediments - the oldest recovered sediments dated to 10.2 ka BP, suggesting that a considerably longer core would have needed to be obtained in order to yield sediments dating to ~17.5 ka BP.

5.4.2. Antarctic Cold Reversal (ACR)

It should be mentioned, that an extrapolated time frame between 31 and 12 ka BP for the onset of AF2-A sedimentation may not only support an origin of the upper portions of AF1 as LLGM till. Instead, the time frame also covers part of the ACR, a renewed cold period associated with a temperature drop of 2–3 °C (Bakke et al., 2021) and significant glacier advance on the north-eastern side of South Georgia (Graham et al., 2017; Bakke et al., 2021). This could mean that the 3rd generation till actually represents glacial deposits from this renewed cold period, while the 2nd generation would be related to the LLGM. Indeed, a number of arguments could potentially support a more extensive ACR advance in JTS than elsewhere: (i) a previous interpretation that ACR advances were restricted to the fjord regions was predominantly based on bathymetry, supplemented with terrestrial age data, from the major fjords around South Georgia (Bentley et al., 2007; Hodgson et al., 2014a). Although this included King Haakon Bay, the JTS tributaries appear to be morphologically very different and their seemingly flat and wide bathymetry (see Fig. 1c and section 2) might have facilitated more extensive glacier advance due to reduced lateral drag. (ii) Most of the major fjords used for the ACR reconstructions are located on the northern side of the island, but a north-south climate gradient across South Georgia actually favours precipitation, and potentially associated larger glacier extents, in the south (Gordon et al., 2008; Cook et al., 2010; Farías-Barahona et al., 2020; Lešić et al., 2022). (iii) Reliable age control for marine ACR deposits exists only from Royal Bay Trough and Cumberland Bay (RBT and CB, respectively; Fig. 1b), where onset of glacimarine sedimentation post-ACR was dated to 13.3 cal ka BP (Graham et al., 2017). (iv) A bathymetric ridge feature in Drygalski Trough (R4) could potentially derive from a more extensive ACR advance, despite the fact that this was considered less likely (Lešić et al., 2022). (v) The large bathymetric high separating AT from JT, BH1, was actually interpreted as a morainal bank or ridge by Graham et al. (2008), which would be a feasible interpretation when considering ACR re-advance.

Despite the above, we actually consider such an extensive ACR advance improbable. This is mainly based on the presence of the uppermost portion of AF1 all the way to the shelf edge, which seems highly unlikely for the ACR. Neither has there been a record of a grounded ice sheet even as far as the mid-shelf during the ACR. Furthermore, the bathymetric data currently available from the KHTS tributaries have a low resolution (GEBCO Compilation Group, 2023), which, on the one hand might indicate that the morphological assessment of the embayments is inaccurate, and on the other could easily fail to represent any potential fjord moraines relating to the ACR. In addition to that, AF2-A was actually interpreted to include the ACR (Lešić et al., 2024), as a corresponding sediment layer in Drygalski Trough seemed to record the ACR only through an increase in sedimentation rates. Otherwise, the sediments were found to be remarkably similar to post-LLGM deposits, i. e. characterised by acoustic stratification and a composition of predominantly (glaci-)marine mud (Lešić et al., 2022). Lastly, symmetry, large height, and steep flanks of BH1 seem to be at odds with an interpretation as a terminal moraine. Instead, based on its E-W orientation, the previously established connection of JTS to the CBSZ, and the much rougher appearance compared to other glacial landforms identified in this study, we consider it more likely that BH1 actually represents a bedrock high.

5.4.3. Post-ACR

The acoustic profiles from the mid- and inner shelf demonstrate that after the ACR, acoustically stratified, post-glacial (glaci-)marine basin-fill sediments (AF2) were deposited onto the pre-existing (post-)glacial deposits, i.e. AF1 and, potentially, the deeper parts of AF2-A. These sediments recorded several distinct changes in depositional environments throughout the Holocene, which are subject of Lešić et al. (2024).

6. Conclusions

Seafloor bathymetry and sub-bottom profiles from the King Haakon Trough System offer new insights into the glacial evolution of a large cross-shelf trough system on the southern South Georgia continental shelf. The data confirm an interpretation of a N–S-oriented main trough, King Haakon Trough (KHT), as a typical cross-shelf trough, formed by glacial erosion, preferentially on its western side, throughout consecutive glacial periods. Its tributary trough system, the Jacobsen Trough System (JTS), also formed from glacial erosion. However, its unusual E-W orientation suggests that its development was probably largely controlled by an adjacent tectonic boundary, the Cooper Bay Shear Zone, causing considerable structural weaknesses in the pre-existing bedrock.

Several glacial landforms visible on the contemporary seafloor allow for the reconstruction of two main trunk glaciers, conjoining on the inner shelf to form an accelerating ice stream. Ice flow direction is indicated by streamlined seafloor, and was shown to be E-W through JTS and roughly N–S through KHT. Progressive elongation of streamlined seafloor and individual crag- and tails on the inner and mid-shelf into longer sedimentary glacial lineations on the outer shelf implies both flow acceleration and a potential change in ice stream substrate along the trough. A GZW is present at the shelf edge, while recessional moraines and morainal banks occur on the outer and mid-shelf. The shallower areas of the seafloor are intensively iceberg-scoured. Together with several stacked till sequences observed in the sub-bottom profiler data, these landforms reveal that during at least one peak glaciation the South Georgia Ice Cap reached all the way to the shelf break, from where it retreated in a step-wise manner predominantly by iceberg-calving. Interestingly, the latest LLGM glaciation seems to have been slightly less extensive than previous ice advances, reaching only until ~1 km from the shelf edge. This might suggest that South Georgia behaved similarly to the other sub-Antarctic islands and that, during MIS 3, the Polar Front was located significantly further north than at present. Interestingly, our data, their comparability to other trough systems around South Georgia, and their potential implications for an early LLGM prior to ~30 ka BP, also suggest that, at least during the LLGM, South Georgia's glacial evolution was similar to that observed on the Antarctic Peninsula. Accordingly, it seems reasonable to assume that the latitudinal position of the Polar Front may have been quite variable over time.

Although the onset of deglaciation is difficult to determine, several arguments are in favour of a similar evolution to both the adjacent Drygalski Trough as well as Royal Bay Trough in NE South Georgia, where ice retreat was already underway by 17.5 ka BP. The data elucidate a further piece of South Georgia's glacial history, but also call for further investigations and, most importantly, chronological information from the marine environment, to be able to fully reconstruct the Quaternary evolution of this sub-Antarctic ice cap.

CRediT authorship contribution statement

Katharina Teresa Streuff: Conceptualization, Investigation, Formal analysis, Data curation, Writing – original draft, Writing – review & editing, Visualization. **Nina-Marie Lešić:** Investigation, Formal analysis, Writing – original draft, Writing – review & editing, Data curation. **Gerhard Kuhn:** Project administration, Funding acquisition, Writing – review & editing. **Miriam Römer:** Data curation, Funding acquisition,

Writing – review & editing. **Sabine Kasten:** Project administration, Data curation, Funding acquisition, Writing – review & editing. **Gerhard Bohrmann:** Project administration, Data curation, Funding acquisition.

Data availability

Data will be made available on request.

References

Anderson, J.B., Conway, H., Bart, P.J., Witus, A.E., Greenwood, S.L., McKay, R.M., Hall, B.L., Ackert, R.P., Licht, K.J., Jakobsson, M., Stone, J.O., 2014. Ross Sea paleo-ice sheet drainage and deglacial history during and since the LGM. Quat. Sci. Rev. 100, 31–54. https://doi.org/10.1016/j.quascirev.2013.08.020.

Andreassen, K., Laberg, J., Vorren, T., 2008. Seafloor geomorphology of the SW Barents Sea and its glaci-dynamic implications. Geomorphology 97, 157–177. https://doi.org/10.1016/j.geomorph.2007.02.050M4.

Andreassen, K., Winsborrow, M., Bjarnadóttir, L., Rüther, D., 2014. Ice stream retreat dynamics inferred from an assemblage of landforms in the northern Barents Sea. Quat. Sci. Rev. 92, 246–257. https://doi.org/10.1016/j.quascirev.2013.09.015M4-Citavi.

Arndt, J.E., Forwick, M., 2016. Deep-water iceberg ploughmarks on hovgaard ridge, fram strait. Geological Society, London, Memoirs 46, 285–286. https://doi.org/10.1144/m46.100.

Arndt, J.E., Jokat, W., Dorschel, B., 2017. The last glaciation and deglaciation of the Northeast Greenland continental shelf revealed by hydro-acoustic data. Quat. Sci. Rev. 160, 45–56. https://doi.org/10.1016/j.quascirev.2017.01.018.

Arndt, J.E., Jokat, W., Dorschel, B., Myklebust, R., Dowdeswell, J.A., Evans, J., 2015. A new bathymetry of the Northeast Greenland continental shelf: constraints on glacial and other processes. G-cubed 16, 3733–3753. https://doi.org/10.1002/2015gc005931.

Bakke, J., Paasche, Ø., Schaefer, J.M., Timmermann, A., 2021. Long-term demise of sub-Antarctic glaciers modulated by the Southern Hemisphere Westerlies. Sci. Rep. 11, 1–10. https://doi.org/10.1038/s41598-021-87317-5.

Barlow, N.L.M., Bentley, M.J., Spada, G., Evans, D.J.A., Hansom, J.D., Brader, M.D., White, D.A., Zander, A., Berg, S., 2016. Testing models of ice cap extent, South Georgia, sub-Antarctic. Quat. Sci. Rev. 154, 157–168. https://doi.org/10.1016/j.quascirev.2016.11.007.

Barnes, D.K.A., Sands, C.J., Hogg, O.T., Robinson, B.J.O., Downey, R.V., Smith, J.A., 2016. Biodiversity signature of the last glacial maximum at South Georgia, Southern Ocean. J. Biogeogr. 43, 2391–2399. https://doi.org/10.1111/jbi.12855.

Barnes, P., Lien, R., 1988. Icebergs rework shelf sediments to 500 m off Antarctica. Geology 16, 1130–1133. https://doi.org/10.1130/0091-7613(1988). M4 - Citavi.

Batchelor, C.L., Dowdeswell, J.A., 2015. Ice-sheet grounding-zone wedges (GZWs) on high-latitude continental margins. Mar. Geol. 363, 65–92. https://doi.org/10.1016/j.margeo.2015.02.001.

Bentley, M.J., Evans, D.J.A., Fogwill, C., Hansom, J., Sugden, D., Kubik, P., 2007. Glacial geomorphology and chronology of deglaciation, South Georgia, sub-Antarctic. Quat. Sci. Rev. 26, 644–677. https://doi.org/10.1016/j.quascirev.2006.11.019.

Bentley, M.J., Ó Cofaigh, C., Anderson, J.B., Conway, H., Davies, B., Graham, A.G.C., Hillenbrand, C.-D., Hodgson, D.A., Jamieson, S.S.R., Larter, R.D., Mackintosh, A., Smith, J.A., Verleyen, E., Ackert, R.P., Bart, P.J., Berg, S., Brunstein, D., Canals, M., Colhoun, E.A., Crosta, X., Dickens, W.A., Domack, E.W., Dowdeswell, J.A., Dunbar, R., Ehrmann, W., Evans, J., Favier, V., Fink, D., Fogwill, C.J., Glasser, N.F., Gohl, K., Golledge, N.R., Goodwin, I., Gore, D.B., Greenwood, S.L., Hall, B.L., Hall, K., Hedding, D.W., Hein, A.S., Hocking, E.P., Jakobsson, M., Johnson, J.S., Jomelli, V., Jones, R.S., Klages, J.P., Kristoffersen, Y., Kuhn, G., Leventer, A., Licht, K.J., Lilly, K., Lindow, J., Livingstone, S.J., Massé, G., McGlone, M.S., McKay, R.M., Melles, M., Miura, H., Mulvaney, R., Nel, W., Nitsche, F.O., O'Brien, P. E., Post, A.L., Roberts, S.J., Saunders, K.M., Selkirk, P.M., Simms, A.R., Spiegel, C., Stolldorf, T.D., Sugden, D.E., van der Putten, N., van Ommen, T., Verfaillie, D., Vyverman, W., Wagner, B., White, D.A., Witus, A.E., Zwartz, D., 2014. A community-based geological reconstruction of antarctic ice sheet deglaciation since the last glacial maximum. Quat. Sci. Rev. 100, 1–9. https://doi.org/10.1016/j.quascirev.2014.06.025.

Berg, S., White, D.A., Jivcov, S., Melles, M., Leng, M.J., Rethemeyer, J., Allen, C., Perren, B., Bennike, O., Viehberg, F., 2019. Holocene glacier fluctuations and environmental changes in subantarctic South Georgia inferred from a sediment record from a coastal inlet. Quat. Res. 91, 132–148. https://doi.org/10.1017/qua.2018.85.

Bianchi, C., Gersonde, R., 2004. Climate evolution at the last deglaciation: the role of the Southern Ocean. Earth Planet Sci. Lett. 228, 407–424. https://doi.org/10.1016/j.epsl.2004.10.003.

Blunier, T., Brook, E.J., 2001. Timing of millennial-scale climate change in Antarctica and Greenland during the last glacial period. Science 291, 109–112. https://doi.org/10.1126/science.291.5501.109.

Bohrmann, G., Aromokeye, A.D., Bihler, V., Dehning, K., Dohrmann, I., Gentz, T., Grahs, M., Hogg, O., Hüttich, D., Kasten, S., Kirschenmann, E., Lange, M., Leymann, T., Linse, K., Loher, M., Malnati, J., Mau, S., Mickoleit, A., Nowald, N., Pape, T., Reuter, C., Rohleder, C., Römer, M., Sahling, H., Stange, N., Torres, M., Vittori, V., von Dobeneck, T., von Neuhoff, H., Weinrebe, W., Wintersteller, P., 2017. R/V METEOR cruise report M134 - emissions of free gas from cross-shelf troughs of South Georgia: distribution, quantification, and sources for methane ebullition sites in Sub-Antarctic waters. Berichte aus dem MARUM und dem. Fachbereich Geowissenschaften der Universität Bremen. MARUM und Fachbereich Geowissenschaften der. Universität Bremen, Bremen, Germany, p. 220. http://nbn-resolving.de/urn:nbn:de:gbv:46-00106081-12.

Bradwell, T., Stoker, M.S., Golledge, N.R., Wilson, C.K., Merritt, J.W., Long, D., Everest, J.D., Hestvik, O.B., Stevenson, A.G., Hubbard, A.L., Finlayson, A.G., Mathers, H.E., 2008. The northern sector of the last British Ice Sheet: maximum extent and demise. Earth Sci. Rev. 88, 207–226.

Broecker, W.S., 1998. Paleocean circulation during the Last Deglaciation: a bipolar seesaw? Paleoceanogr. Paleoclimatol. 13, 119–121.

Brouard, E., Lajeunesse, P., 2017. Maximum extent and decay of the Laurentide Ice Sheet in western Baffin Bay during the last glacial episode. Sci. Rep. 7, 10711 https://doi.org/10.1038/s41598-017-11010-9.

Camerlenghi, A., Rebesco, M., Accettella, D., 2016. Storfjorden Trough-mouth fan, Barents Sea margin. Geological Society 46, 371–372. https://doi.org/10.1144/m46.33. London, Memoirs.

Caress, D.W., Chayes, D.N., 2017. MB-system: Mapping the Seafloor. https://www.mbari.org/products/,pp.research-software/mb-system.

Clapperton, C.M., Sugden, D.E., Birnie, J., Wilson, M.J., 1989. Late-glacial and Holocene glacier fluctuations and environmental change on SouthSouth Georgia, Southern Ocean. Quat. Res. 31, 210–228. https://doi.org/10.1016/0033-5894(89)90006-9.

Clark, C.D., Hughes, A.L.C., Greenwood, S.L., Jordan, C., Sejrup, H.P., 2012. Pattern and timing of retreat of the last British-Irish Ice Sheet. Quat. Sci. Rev. 44, 112–146. https://doi.org/10.1016/j.quascirev.2010.07.019M4-Citavi.

Clark, P.U., Dyke, A.S., Shakun, J.D., Carlson, A.E., Clark, J., Wohlfarth, B., Mitrovica, J. X., Hostetler, S.W., McCabe, A.M., 2009. The last glacial maximum. Science 325, 710–714. https://doi.org/10.1126/science.1172873.

Clayton, L.E.E., Teller, J.T., Attig, J.W., 1985. Surging of the southwestern part of the laurentide ice sheet. Boreas 14, 235–241. https://doi.org/10.1111/j.1502-3885.1985.tb00726.x.

Cook, A.J., Poncet, S., Cooper, A.P.R., Herbert, D.J., Christie, D., 2010. Glacier retreat on South Georgia and implications for the spread of rats. Antarct. Sci. 22, 255–263. https://doi.org/10.1017/S0954102010000064.

Copland, L., Sharp, M.J., Dowdeswell, J.A., 2003. The distribution and flow characteristics of surge-type glaciers in the Canadian High Arctic. Ann. Glaciol. 36, 73–81. https://doi.org/10.3189/172756403781816301.

Dalziel, I.W.D., Macdonald, D.I.M., Stone, P., Storey, B.C., 2021. South Georgia microcontinent: displaced fragment of the southernmost Andes. Earth Sci. Rev. 220 https://doi.org/10.1016/j.earscirev.2021.103671.

Darvill, C.M., Bentley, M.J., Stokes, C.R., Hein, A.S., Rodés, Á., 2015. Extensive MIS 3 glaciation in southernmost Patagonia revealed by cosmogenic nuclide dating of outwash sediments. Earth Planet Sci. Lett. 429, 157–169. https://doi.org/10.1016/j.epsl.2015.07.030.

Darvill, C.M., Bentley, M.J., Stokes, C.R., Shulmeister, J., 2016. The timing and cause of glacial advances in the southern mid-latitudes during the last glacial cycle based on a synthesis of exposure ages from Patagonia and New Zealand. Quat. Sci. Rev. 149, 200–214. https://doi.org/10.1016/j.quascirev.2016.07.024.

Dowdeswell, J.A., Bamber, J.L., 2007. Keel depths of modern Antarctic icebergs and implications for sea-floor scouring in the geological record. Mar. Geol. 243, 120–131. https://doi.org/10.1016/j.margeo.2007.04.008.

Dowdeswell, J.A., Canals, M., Jakobsson, M., Todd, B.J., Dowdeswell, E.K., Hogan, K.A., 2016a. The variety and distribution of submarine glacial landforms and implications

for ice-sheet reconstruction. Geological Society, London, Memoirs 46, 519–552. https://doi.org/10.1144/m46.183.

Dowdeswell, J.A., Jakobsson, M., Hogan, K.A., O'Regan, M., Backman, J., Evans, J., Hell, B., Löwemark, L., Marcussen, C., Noormets, R., Ó Cofaigh, C., Sellén, E., Sölvsten, M., 2010. High-resolution geophysical observations of the Yermak Plateau and northern Svalbard margin: implications for ice-sheet grounding and deep-keeled icebergs. Quat. Sci. Rev. 29, 3518–3531. https://doi.org/10.1016/j.quascirev.2010.06.002.

Dowdeswell, J.A., Ó Cofaigh, C., Noormets, R., Larter, R.D., Hillenbrand, C.-D., Benetti, S., Evans, J., Pudsey, C.J., 2008a. A major trough-mouth fan on the continental margin of the Bellingshausen Sea, West Antarctica: the Belgica Fan. Mar. Geol. 252, 129–140. https://doi.org/10.1016/j.margeo.2008.03.017.

Dowdeswell, J.A., Ó Cofaigh, C., Pudsey, C.J., 2004. Continental slope morphology and sedimentary processes at the mouth of an Antarctic palaeo-ice stream. Mar. Geol. 204, 203–214. https://doi.org/10.1016/s0025-3227(03)00338-4.

Dowdeswell, J.A., Ottesen, D., Bellec, V.K., 2020. The changing extent of marine-terminating glaciers and ice caps in northeastern Svalbard since the 'Little Ice Age' from marine-geophysical records. Holocene 30, 389–401. https://doi.org/10.1177/0959683619887429.

Dowdeswell, J.A., Ottesen, D., Evans, J., Ó Cofaigh, C., Anderson, J.B., 2008b. Submarine glacial landforms and rates of ice-stream collapse. Geology 36, 819. https://doi.org/10.1130/g24808a.1.

Dowdeswell, J.A., Ottesen, D., Rise, L., 2016b. Landforms characteristic of inter-ice stream settings on the Norwegian and Svalbard continental margins. Geological Society, London, Memoirs 46, 437–444. https://doi.org/10.1144/m46.164.

Dowdeswell, J.A., Ottesen, D., Rise, L., Craig, J., 2007. Identification and preservation of landforms diagnostic of past ice-sheet activity on continental shelves from three-dimensional seismic evidence. Geology 35, 359. https://doi.org/10.1130/g23200a.1.

Evans, J., Dowdeswell, J.A., Ó Cofaigh, C., 2004. Late Quaternary submarine bedforms and ice-sheet flow in Gerlache Strait and on the adjacent continental shelf, Antarctic Peninsula. J. Quat. Sci. 19, 397–407. https://doi.org/10.1002/jqs.831.

Evans, J., Dowdeswell, J.A., Ó Cofaigh, C., Benham, T.J., Anderson, J.B., 2006. Extent and dynamics of the west antarctic ice sheet on the outer continental shelf of pine island bay during the last glaciation. Mar. Geol. 230, 53–72. https://doi.org/10.1016/j.margeo.2006.04.001.

Evans, J., Pudsey, C.J., Ó Cofaigh, C., Morris, P., Domack, E.W., 2005. Late Quaternary glacial history, flow dynamics and sedimentation along the eastern margin of the Antarctic Peninsula Ice Sheet. Quat. Sci. Rev. 24, 741–774. https://doi.org/10.1016/j.quascirev.2004.10.007.

Farías-Barahona, D., Sommer, C., Sauter, T., Bannister, D., Seehaus, T., Malz, P., Casassa, G., Mayewski, P., Turton, J., Braun, M., 2020. Detailed quantification of glacier elevation and mass changes in South Georgia. Environ. Res. Lett. 15 https://doi.org/10.1088/1748-9326/ab6b32.

Farnsworth, W.R., Ingólfsson, Ó., Retelle, M., Schomacker, A., 2016. Over 400 previously undocumented Svalbard surge-type glaciers identified. Geomorphology 264, 52–60. https://doi.org/10.1016/j.geomorph.2016.03.025.

Forwick, M., Vorren, T.O., 2009. Late weichselian and Holocene sedimentary environments and ice rafting in isfjorden, spitsbergen. Palaeogeogr. Palaeoclimatol. Palaeoecol. 280, 258–274. https://doi.org/10.1016/j.palaeo.2009.06.026.

Forwick, M., Vorren, T.O., 2011. Stratigraphy and deglaciation of the isfjorden area, spitsbergen. Norw. J. Geol. 90, 163–179.

Forwick, M., Vorren, T.O., Hald, M., Korsun, S., Roh, Y., Vogt, C., Yoo, K., 2010. Spatial and temporal influence of glaciers and rivers on the sedimentary environment in Sassenfjorden and Tempelfjorden, Spitsbergen. In: Howe, J., Austin, W., Forwick, M., Paetzel, M. (Eds.), Geol Soc Spec Publ. Geological Society, London, London, pp. 163–193. https://doi.org/10.1144/SP344.13M4-Citavi.

GEBCO Compilation Group, 2023. General Bathymetric Chart of the Oceans 2023 Grid.

Geprägs, P., Torres, M.E., Mau, S., Kasten, S., Römer, M., Bohrmann, G., 2016. Carbon cycling fed by methane seepage at the shallow Cumberland Bay, South Georgia, sub-Antarctic. G-cubed 17, 1401–1418. https://doi.org/10.1002/2016gc006276.

Gordon, J.E., Haynes, V.M., Hubbard, A., 2008. Recent glacier changes and climate trends on South Georgia. Global Planet. Change 60, 72–84. https://doi.org/10.1016/j.gloplacha.2006.07.037.

Graham, A.G.C., Fretwell, P.T., Larter, R.D., Hodgson, D.A., Wilson, C.K., Tate, A.J., Morris, P., 2008. A new bathymetric compilation highlighting extensive paleo-ice sheet drainage on the continental shelf, South Georgia, sub-Antarctica. G-cubed 9, 1–21. https://doi.org/10.1029/2008gc001993.

Graham, A.G.C., Kuhn, G., Meisel, O., Hillenbrand, C.-D., Hodgson, D.A., Ehrmann, W., Wacker, L., Wintersteller, P., dos Santos Ferreira, C., Römer, M., White, D.A., Bohrmann, G., 2017. Major advance of South Georgia glaciers during the Antarctic Cold Reversal following extensive sub-Antarctic glaciation. Nat. Commun. 8, 14798 https://doi.org/10.1038/ncomms14798.

Graham, A.G.C., Larter, R.D., Gohl, K., Hillenbrand, C.-D., Smith, J.A., Kuhn, G., 2009. Bedform signature of a West Antarctic palaeo-ice stream reveals a multi-temporal record of flow and substrate control. Quat. Sci. Rev. 28, 2774–2793.

Hillenbrand, C.-D., Bentley, M.J., Stolldorf, T.D., Hein, A.S., Kuhn, G., Graham, A.G.C., Fogwill, C.J., Kristoffersen, Y., Smith, J.A., Anderson, J.B., Larter, R.D., Melles, M., Hodgson, D.A., Mulvaney, R., Sugden, D.E., 2014. Reconstruction of changes in the weddell sea sector of the antarctic ice sheet since the last glacial maximum. Quat. Sci. Rev. 100, 111–136. https://doi.org/10.1016/j.quascirev.2013.07.020.

Hodgson, D.A., Graham, A.G.C., Griffiths, H.J., Roberts, S.J., Ó Cofaigh, C., Bentley, M.J., Evans, D.J.A., 2014a. Glacial history of sub-Antarctic South Georgia based on the submarine geomorphology of its fjords. Quat. Sci. Rev. 89, 129–147. https://doi.org/10.1016/j.quascirev.2013.12.005.

Hodgson, D.A., Graham, A.G.C., Roberts, S.J., Bentley, M.J., Ó Cofaigh, C., Verleyen, E., Vyverman, W., Jomelli, V., Favier, V., Brunstein, D., Verfaillie, D., Colhoun, E.A., Saunders, K.M., Selkirk, P.M., Mackintosh, A., Hedding, D.W., Nel, W., Hall, K., McGlone, M.S., van der Putten, N., Dickens, W.A., Smith, J.A., 2014b. Terrestrial and submarine evidence for the extent and timing of the Last Glacial Maximum and the onset of deglaciation on the maritime-Antarctic and sub-Antarctic islands. Quat. Sci. Rev. 100, 137–158. https://doi.org/10.1016/j.quascirev.2013.12.001.

Hogan, K.A., Dix, J.K., Lloyd, J.M., Long, A.J., Cotterill, C.J., 2011. Seismic stratigraphy records the deglacial history of Jakobshavn Isbræ, West Greenland. J. Quat. Sci. 26, 757–766. https://doi.org/10.1002/jqs.1500.

Hogg, O.T., Huevenne, V.A., Griffiths, H.J., Dorschel, B., Linse, K., 2017. A Bathymetric Compilation of South Georgia, 1985-2015 (Version 1.0) Polar Data Centre. British Antarctic Survey, Natural Environment Research Council, Cambridge. CB3 0ET, UK.

Hogg, O.T., Huevenne, V.A., Griffiths, H.J., Dorschel, B., Linse, K., 2016. Landscape mapping at sub-Antarctic South Georgia provides a protocol for underpinning large-scale marine protected areas. Sci. Rep. 6, 33163 https://doi.org/10.1038/srep33163.

Holland, D.M., Thomas, R.H., de Young, B., Ribergaard, M.H., Lyberth, B., 2008. Acceleration of Jakobshavn Isbræ triggered by warm subsurface ocean waters. Nat. Geosci. 1, 659–664. https://doi.org/10.1038/ngeo316.

Hughes, A.L.C., Gyllencreutz, R., Lohne, Ø.S., Mangerud, J., Svendsen, J.I., 2016. The last Eurasian ice sheets - a chronological database and time-slice reconstruction, DATED-1. Boreas 45, 1–45. https://doi.org/10.1111/bor.12142M4-Citavi.

Hunter, L.E., Powell, R.D., Lawson, D.E., 1996. Morainal-bank sediment budgets and their influence on the stability of tidewater termini of valley glaciers entering Glacier Bay, Alaska, U.S.A. Ann. Glaciol. 22, 211–216. https://doi.org/10.3189/1996AoG22-1-211-216.

Jomelli, V., Schimmelpfennig, I., Favier, V., Mokadem, F., Landais, A., Rinterknecht, V., Brunstein, D., Verfaillie, D., Legentil, C., Aumaitre, G., Bourlès, D.L., Keddadouche, K., 2018. Glacier extent in sub-Antarctic Kerguelen archipelago from MIS 3 period: Evidence from ^{36}Cl dating. Quat. Sci. Rev. 183, 110–123. https://doi.org/10.1016/j.quascirev.2018.01.008.

Kaplan, M.R., Fogwill, C.J., Sugden, D.E., Hulton, N.R.J., Kubik, P.W., Freeman, S.P.H.T., 2008. Southern Patagonian glacial chronology for the Last Glacial period and implications for Southern Ocean climate. Quat. Sci. Rev. 27, 284–294.

Kaplan, M.R., Schaefer, J.M., Strelin, J.A., Denton, G.H., Anderson, R.F., Vandergoes, M.J., Finkel, R.C., Schwartz, R., Travis, S.G., Garcia, J.L., Martini, M.A., Nielsen, S.H.H., 2016. Patagonian and southern South Atlantic view of Holocene climate. Quat. Sci. Rev. 141, 112–125. https://doi.org/10.1016/j.quascirev.2016.03.014.

Kasten, S., 2023. The Expedition PS133/2 of the Research Vessel POLARSTERN to the Scotia Sea in 2022. In: Bornemann, H., Amir Sawadkuhi, S. (Eds.), Berichte zur Polar- und Meeresforschung/Reports on polar and marine research. Alfred-Wegener-Institut Helmholtz-Zentrum für Polar- und Meeresforschung, p. 183. https://doi.org/10.57738/BzPM_0775_2023. Bremerhaven.

King, E.C., Hindmarsh, R.C.A., Stokes, C.R., 2009. Formation of mega-scale glacial lineations observed beneath a West Antarctic ice stream. Nat. Geosci. 2, 585–588. https://doi.org/10.1038/ngeo581.

Klages, J.P., Kuhn, G., Graham, A.G.C., Hillenbrand, C.-D., Smith, J.A., Nitsche, F.O., Larter, R.D., Gohl, K., 2015. Palaeo-ice stream pathways and retreat style in the easternmost Amundsen Sea Embayment, West Antarctica, revealed by combined multibeam bathymetric and seismic data. Geomorphology 245, 207–222. https://doi.org/10.1016/j.geomorph.2015.05.020.

Kuhn, G., Hillenbrand, C.-D., Kasten, S., Smith, J.A., Nitsche, F.O., Frederichs, T., Wiers, S., Ehrmann, W., Klages, J.P., Mogollón, J.M., 2017. Evidence for a palaeo-subglacial lake on the Antarctic continental shelf. Nat. Commun. 8, 15591 https://doi.org/10.1038/ncomms15591.

Laberg, J.S., Vorren, T.O., 1995. Late Weichselian submarine debris flow deposits on the Bear Island Trough Mouth Fan. Mar. Geol. 127, 45–72. https://doi.org/10.1016/0025-3227(95)00055-4.

Larter, R.D., Anderson, J.B., Graham, A.G.C., Gohl, K., Hillenbrand, C.-D., Jakobsson, M., Johnson, J.S., Kuhn, G., Nitsche, F.O., Smith, J.A., Witus, A.E., Bentley, M.J., Dowdeswell, J.A., Ehrmann, W., Klages, J.P., Lindow, J., Ó Cofaigh, C., Spiegel, C., 2014. Reconstruction of changes in the Amundsen Sea and Bellingshausen Sea sector of the West Antarctic Ice Sheet since the Last Glacial Maximum. Quat. Sci. Rev. 100, 55–86. https://doi.org/10.1016/j.quascirev.2013.10.016.

Lešić, N.-M., 2024. Climate-driven Holocene sedimentation in King Haakon Trough System, sub-Antarctic South Georgia, in: Late Pleistocene and Holocene sediments around South Georgia: Archives for climate-induced signals in sub-Antarctica since the last glaciation, Doctoral dissertation, University of Bremen, Bremen, Germany. DOI: https://doi.org/10.26092/elib/2890.

Lešić, N.-M., Streuff, K.T., Bohrmann, G., Kasten, S., Kuhn, G., 2024. Spatial and temporal variability in Holocene trough-fill sediments, King Haakon Trough System, sub-Antarctic South Georgia Quaternary. Sci. Adv. 13, 100156 https://doi.org/10.1016/j.qsa.2023.100156.

Lešić, N.-M., Streuff, K.T., Bohrmann, G., Kuhn, G., 2022. Glacimarine sediments from outer Drygalski Trough, sub-Antarctic South Georgia – evidence for extensive glaciation during the Last Glacial Maximum. Quat. Sci. Rev. 292 https://doi.org/10.1016/j.quascirev.2022.107657.

Licht, K.J., Dunbar, N.W., Andrews, J.T., Jennings, A.E., 1999. Distinguishing subglacial till and glacial marine diamictons in the western Ross Sea, Antarctica: Implications for a last glacial maximum grounding line. GSA Bulletin 111, 91–103. https://doi.org/10.1130/0016-7606(1999)111<0091:Dstagm>2.3.Co;2.

Lucchi, R.G., Pedrosa, M.T., Camerlenghi, A., Urgeles, R., de Mol, B., Rebesco, M., 2012. Recent submarine landslides on the continental slope of Storfjorden and Kveithola Trough-Mouth Fans (northwest Barents Sea). In: Yamada, Y., Kawamura, K., Ikehara, K., Ogawa, Y., Urgeles, R., Mosher, D., Chaytor, J., Strasser, M. (Eds.),

Submarine Mass Movements and Their Consequences. Springer, Netherlands, Dordrecht, pp. 735–745. https://doi.org/10.1007/978-94-007-2162-3_65.

Macdonald, D.I.M., Storey, B.C., 1987. South Georgia. In: Thomson, J.W. (Ed.), BAS GEOMAP Series. British Antarctic Survey and National Environmental Research Council. Cambridge, UK.

Mackintosh, A.N., Verleyen, E., O'Brien, P.E., White, D.A., Jones, R.S., McKay, R., Dunbar, R., Gore, D.B., Fink, D., Post, A.L., Miura, H., Leventer, A., Goodwin, I., Hodgson, D.A., Lilly, K., Crosta, X., Golledge, N.R., Wagner, B., Berg, S., van Ommen, T., Zwartz, D., Roberts, S.J., Vyverman, W., Masse, G., 2014. Retreat history of the East Antarctic Ice Sheet since the Last Glacial Maximum. Quat. Sci. Rev. 100, 10–30. https://doi.org/10.1016/j.quascirev.2013.07.024.

MacLean, B., Blasco, S., Bennett, R., Hughes Clarke, J.E., Patton, E., 2016. Crag-and-tail features, Amundsen Gulf, Canadian Arctic Archipelago. In: Dowdeswell, J.A., Canals, M., Jakobsson, M., Todd, B.J., Dowdeswell, E.K., Hogan, K.A. (Eds.), Geol Soc Mem. The Geological Society of London, pp. 53–54. https://doi.org/10.1144/m46.84.

Matano, R.P., Combes, V., Young, E.F., Meredith, M.P., 2020. Modeling the impact of ocean circulation on chlorophyll blooms around South Georgia, Southern Ocean. J. Geophys. Res. Oceans 125, e2020JC016391. https://doi.org/10.1029/2020jc016391.

Meier, M., Post, A., 1969. What are glacier surges? Can. J. Earth Sci. 6, 807–817. https://doi.org/10.1139/e69-081M4-Citavi.

Moreno, P.I., Vilanova, I., Villa-Martinez, R., Dunbar, R.B., Mucciarone, D.A., Kaplan, M. R., Garreaud, R.D., Rojas, M., Moy, C.M., De Pol-Holz, R., Lambert, F., 2018. Onset and evolution of Southern Annular Mode-like changes at centennial timescale. Sci. Rep. 8, 3458. https://doi.org/10.1038/s41598-018-21836-6.

Murray, T., Scharrer, K., James, T.D., Dye, S.R., Hanna, E., Booth, A.D., Selmes, N., Luckman, A., Hughes, A.L.C., Cook, S., Huybrechts, P., 2010. Ocean regulation hypothesis for glacier dynamics in southeast Greenland and implications for ice sheet mass changes. J. Geophys. Res. 115 https://doi.org/10.1029/2009jf001522.

Ó Cofaigh, C., Andrews, J.T., Jennings, A.E., Dowdeswell, J.A., Hogan, K.A., Kilfeather, A.A., Sheldon, C., 2013. Glacimarine lithofacies, provenance and depositional processes on a West Greenland trough-mouth fan. J. Quat. Sci. 28, 13–26. https://doi.org/10.1002/jqs.2569M4-Citavi.

Ó Cofaigh, C., Davies, B.J., Livingstone, S.J., Smith, J.A., Johnson, J.S., Hocking, E.P., Hodgson, D.A., Anderson, J.B., Bentley, M.J., Canals, M., Domack, E., Dowdeswell, J. A., Evans, J., Glasser, N.F., Hillenbrand, C.-D., Larter, R.D., Roberts, S.J., Simms, A. R., 2014. Reconstruction of ice-sheet changes in the Antarctic Peninsula since the Last Glacial Maximum. Quat. Sci. Rev. 100, 87–110. https://doi.org/10.1016/j.quascirev.2014.06.023.

Ó Cofaigh, C., Dowdeswell, J., Allen, C., Hiemstra, J., Pudsey, C., Evans, J., Evans, D., 2005. Flow dynamics and till genesis associated with a marine-based Antarctic paleo-ice stream. Quat. Sci. Rev. 24, 709–740. https://doi.org/10.1016/j.quascirev.2004.10.006M4-Citavi.

Ó Cofaigh, C., Dowdeswell, J.A., Evans, J., Kenyon, N.H., Taylor, J., Mienert, J., Wilken, M., 2004. Timing and significance of glacially influenced mass-wasting in the submarine channels of the Greenland Basin. Mar. Geol. 207, 39–54. https://doi.org/10.1016/j.margeo.2004.02.009.

Ó Cofaigh, C., Dowdeswell, J.A., Evans, J., Larter, R.D., 2008. Geological constraints on Antarctic palaeo-ice-stream retreat. Earth Surf. Process. Landforms 33, 513–525. https://doi.org/10.1002/esp.1669M4-Citavi.

Ó Cofaigh, C., Dowdeswell, J.A., Grobe, H., 2001. Holocene glacimarine sedimentation, inner Scoresby Sund, East Greenland: the influence of fast-flowing ice-sheet outlet glaciers. Mar. Geol. 175, 103–129. https://doi.org/10.1016/s0025-3227(01)00117-7.

Ó Cofaigh, C., Pudsey, C.J., Dowdeswell, J.A., Morris, P., 2002. Evolution of subglacial bedforms along a paleo-ice stream, Antarctic Peninsula continental shelf. Geophys. Res. Lett. 29, 41, 41-41-44.

Oppedal, L.T., Bakke, J., Paasche, Ø., Werner, J.P., van der Bilt, W.G.M., 2018. Cirque Glacier on South Georgia Shows Centennial Variability over the Last 7000 Years. Front. Earth Sci. 6 https://doi.org/10.3389/feart.2018.00002.

Orsi, A.H., Whitworth, T., Nowlin, W.D., 1995. On the meridional extent and fronts of the Antarctic Circumpolar Current. Deep Sea Res. I Oceanogr. Res. Paper 42, 641–673. https://doi.org/10.1016/0967-0637(95)00021-W.

Ottesen, D., Dowdeswell, J.A., 2006. Assemblages of submarine landforms produced by tidewater glaciers in Svalbard. J. Geophys. Res. 111, 1–16. https://doi.org/10.1029/2005jf000330.

Ottesen, D., Dowdeswell, J.A., 2009. An inter-ice-stream glaciated margin: Submarine landforms and a geomorphic model based on marine-geophysical data from Svalbard. GSA Bulletin 121, 1647–1665. https://doi.org/10.1130/b26467.1.

Ottesen, D., Dowdeswell, J.A., Bellec, V.K., Bjarnadóttir, L.R., 2017. The geomorphic imprint of glacier surges into open-marine waters: examples from eastern Svalbard. Mar. Geol. 392, 1–29.

Ottesen, D., Dowdeswell, J.A., Landvik, J.Y., Mienert, J., 2007. Dynamics of the Late Weichselian ice sheet on Svalbard inferred from high-resolution sea-floor morphology. Boreas 36, 286–306. https://doi.org/10.1080/03009480701210378.

Ottesen, D., Dowdeswell, J.A., Rise, L., 2005. Submarine landforms and the reconstruction of fast-flowing ice streams within a large Quaternary ice sheet: The 2500-km-long Norwegian-Svalbard margin (57°–80°N). Geol. Soc. Am. Bull. 117, 1033. https://doi.org/10.1130/b25577.1.

Post, A., 1969. Distribution of Surging Glaciers in Western North America. J. Glaciol. 8, 229–240. https://doi.org/10.3189/s0022143000031221.

Pritchard, H.D., Ligtenberg, S.R., Fricker, H.A., Vaughan, D.G., van den Broeke, M.R., Padman, L., 2012. Antarctic ice-sheet loss driven by basal melting of ice shelves. Nature 484, 502–505. https://doi.org/10.1038/nature10968.

Pudsey, C.J., Howe, J.A., 1998. Quaternary history of the Antarctic Circumpolar Current: evidence from the Scotia Sea. Mar. Geol. 148, 83–112. https://doi.org/10.1016/S0025-3227(98)00014-0.

Putnam, A.E., Denton, G.H., Schaefer, J.M., Barrell, D.J.A., Andersen, B.G., Finkel, R.C., Schwartz, R., Doughty, A.M., Kaplan, M.R., Schlüchter, C., 2010. Glacier advance in southern middle-latitudes during the Antarctic Cold Reversal. Nat. Geosci. 3, 700–704. https://doi.org/10.1038/ngeo962.

Putnam, A.E., Schaefer, J.M., Denton, G.H., Barrell, D.J.A., Finkel, R.C., Andersen, B.G., Schwartz, R., Chinn, T.J.H., Doughty, A.M., 2012. Regional climate control of glaciers in New Zealand and Europe during the pre-industrial Holocene. Nat. Geosci. 5, 627–630. https://doi.org/10.1038/ngeo1548.

Rignot, E., Jacobs, S., Mouginot, J., Scheuchl, B., 2013. Ice-shelf melting around Antarctica. Science 341, 266–270. https://doi.org/10.1126/science.1235798.

Römer, M., Torres, M., Kasten, S., Kuhn, G., Graham, A.G.C., Mau, S., Little, C.T.S., Linse, K., Pape, T., Geprägs, P., Fischer, D., Wintersteller, P., Marcon, Y., Rethemeyer, J., Bohrmann, G., 2014. First evidence of widespread active methane seepage in the Southern Ocean, off the sub-Antarctic island of South Georgia. Earth Planet Sci. Lett. 403, 166–177. https://doi.org/10.1016/j.epsl.2014.06.036.

Rosqvist, G.C., Rietti-Shati, M., Shemesh, A., 1999. Late glacial to middle Holocene climatic record of lacustrine biogenic silica oxygen isotopes from a Southern Ocean island. Geology 27, 967. https://doi.org/10.1130/0091-7613(1999)027<0967:LGTMHC>2.3.CO;2.

Ryan, J.C., Dowdeswell, J.A., Hogan, K.A., 2016. Three cross-shelf troughs on the continental shelf of SW Greenland from Olex data. In: Dowdeswell, J.A., Canals, M., Jakobsson, M., Todd, B.J., Dowdeswell, E.K., Hogan, K.A. (Eds.), Geol Soc Mem. The Geological Society of London, pp. 167–168. https://doi.org/10.1144/m46.9.

Rydningen, T.A., Vorren, T.O., Laberg, J.S., Kolstad, V., 2013. The marine-based NW Fennoscandian ice sheet: glacial and deglacial dynamics as reconstructed from submarine landforms. Quat. Sci. Rev. 68, 126–141. https://doi.org/10.1016/j.quascirev.2013.02.013.

Shipp, S.S., Anderson, J.B., Domack, E., 1999. Late Pleistocene–Holocene retreat of the West Antarctic Ice-Sheet system in the Ross Sea: Part 1—Geophysical results. Geol. Soc. Am. Bull. 111 https://doi.org/10.1130/0016-7606(1999)111<1486:Lphrot>2.3.Co;2.

Smith, J., 1960. Glacier Problems in South Georgia. J. Glaciol. 3, 705–714. https://doi.org/10.3189/s0022143000018001.

South Georgia GIS, 2023. South Georgia Geographic Information System. British Antarctic Survey.

Spagnolo, M., Clark, C.D., 2009. A geomorphological overview of glacial landforms on the Icelandic continental shelf. J. Maps 5, 37–52. https://doi.org/10.4113/jom.2009.1049.

Spagnolo, M., Clark, C.D., Ely, J.C., Stokes, C.R., Anderson, J.B., Andreassen, K., Graham, A.G.C., King, E.C., 2014. Size, shape and spatial arrangement of mega-scale glacial lineations from a large and diverse dataset. Earth Surf. Process. Landforms 1432–1448. https://doi.org/10.1002/esp.3532.

Stokes, C.R., Clark, C.D., 1999. Geomorphological criteria for identifying Pleistocene ice streams. Ann. Glaciol. 28, 67–74. https://doi.org/10.3189/172756499781821625.

Streuff, K.T., Ó Cofaigh, C., Hogan, K.A., Jennings, A.E., Lloyd, J.M., Noormets, R., Nielsen, T., Kuijpers, A., Dowdeswell, J.A., Weinrebe, W., 2017a. Seafloor geomorphology and glacimarine sedimentation associated with fast-flowing ice sheet outlet glaciers in Disko Bay, West Greenland. Quat. Sci. Rev. 169, 206–230. https://doi.org/10.1016/j.quascirev.2017.05.021.

Streuff, K.T., Ó Cofaigh, C., Noormets, R., Lloyd, J.M., 2017b. Submarine landforms and glacimarine sedimentary processes in Lomfjorden, East Spitsbergen. Mar. Geol. 390, 51–71. https://doi.org/10.1016/j.margeo.2017.04.014.

Streuff, K.T., Ó Cofaigh, C., Noormets, R., Lloyd, J.M., 2018. Submarine landform assemblages and sedimentary processes in front of Spitsbergen tidewater glaciers. Mar. Geol. 402, 209–227. https://doi.org/10.1016/j.margeo.2017.09.006.

Streuff, K.T., Ó Cofaigh, C., Wintersteller, P., 2022. GlaciDat – a GIS database of submarine glacial landforms and sediments in the Arctic. Boreas. https://doi.org/10.1111/bor.12577.

Strother, S.L., Salzmann, U., Roberts, S.J., Hodgson, D.A., Woodward, J., van Nieuwenhuyze, W., Verleyen, E., Vyverman, W., Moreton, S.G., 2015. Changes in Holocene climate and the intensity of Southern Hemisphere Westerly Winds based on a high-resolution palynological record from sub-Antarctic South Georgia. Holocene 25, 263–279. https://doi.org/10.1177/0959683614557576.

Sugden, D.E., Clapperton, C.M., 1977. The maximum ice extent on island groups in the Scotia Sea, Antarctica. Quat. Res. 7, 268–282. https://doi.org/10.1016/0033-5894(77)90041-2.

Taylor, J., Dowdeswell, J.A., Kenyon, N.H., Ó Cofaigh, C., 2002. Late Quaternary architecture of trough-mouth fans: debris flows and suspended sediments on the Norwegian margin. In: Dowdeswell, J.A., Ó Cofaigh, C. (Eds.), Glacier-Influenced Sedimentation on High-Latitude Continental Margins. Geological Society London, London, UK, pp. 55–71. https://doi.org/10.1144/gsl.Sp.2002.203.01.04.

Thomas, G.S.P., Chiverrell, R.C., 2007. Structural and depositional evidence for repeated ice-marginal oscillation along the eastern margin of the Late Devensian Irish Sea Ice Stream. Quat. Sci. Rev. 26, 2375–2405. https://doi.org/10.1016/j.quascirev.2007.06.025.

Tulaczyk, S.M., Scherer, R.P., Clark, C.D., 2001. A ploughing model for the origin of weak tills beneath ice streams: a qualitative treatment. Quat. Int. 86, 59–70. https://doi.org/10.1016/S1040-6182(01)00050-7.

van der Bilt, W.G.M., Bakke, J., Werner, J.P., Paasche, Ø., Rosqvist, G.C., Solheim Vatle, S., 2017. Late Holocene glacier reconstruction reveals retreat behind present limits and two-stage Little Ice Age on subantarctic South Georgia. J. Quat. Sci. 32, 888–901. https://doi.org/10.1002/jqs.2937.

van der Putten, N., Verbruggen, C., 2005. The onset of deglaciation of Cumberland Bay and Stromness Bay, South Georgia. Antarct. Sci. 17, 29–32. https://doi.org/10.1017/S0954102005002397.

van der Putten, N., Verbruggen, C., Ochyra, R., Spassov, S., de Beaulieu, J.L., de Dapper, M., Hus, J., Thouveny, N., 2009. Peat bank growth, Holocene palaeoecology and climate history of South Georgia (sub-Antarctica), based on a botanical macrofossil record. Quat. Sci. Rev. 28, 65–79. https://doi.org/10.1016/j.quascirev.2008.09.023.

Wellner, J.S., Lowe, A.L., Shipp, S.S., Anderson, J.B., 2001. Distribution of glacial geomorphic features on the Antarctic continental shelf and correlation with substrate: implications for ice behavior. J. Glaciol. 47, 397–411. https://doi.org/10.3189/172756501781832043.

White, D.A., Bennike, O., Melles, M., Berg, S., Binnie, S.A., 2017. Was South Georgia covered by an ice cap during the Last Glacial Maximum? Geological Society, London, Special Publications 461, 49–59. https://doi.org/10.1144/sp461.4.

Williams, P.W., McGlone, M.S., Neil, H.L., Zhao, J.-X., 2015. A review of New Zealand palaeoclimate from the Last Interglacial to the global Last Glacial Maximum. Quat. Sci. Rev. 110, 92–106. https://doi.org/10.1016/j.quascirev.2014.12.017.

Wu, S., Lembke-Jene, L., Lamy, F., Arz, H.W., Nowaczyk, N.R., Xiao, W., Zhang, X., Hass, H.C., Titschack, J., Zheng, X., Liu, J., Dumm, L., Diekmann, B., Nürnberg, D., Tiedemann, R., Kuhn, G., 2021. Orbital- and millennial-scale Antarctic Circumpolar Current variability in Drake Passage over the past 140,000 years. Nat. Commun. 12, 1–9. https://doi.org/10.1038/s41467-021-24264-9.